THE JOURNAL OF PHYSICAL CHEMISTRY C

pubs.acs.org/JPCC

Perspective

Progress and Prospects of Solution-Processed Two-Dimensional Semiconductor Nanocrystals

Dmitry Porotnikov and Mikhail Zamkov*

Cite This: J. Phys. Chem. C 2020, 124, 21895−21908

Read Online

ACCESS | Metrics & More | Article Recommendations

ABSTRACT: Two-dimensional (2D) semiconductor nanocrystals processed from solution have become an attractive material platform for the development of optoelectronic devices. The synergy of the 2D charge carrier confinement and soft fabrication methods has enabled new paradigms in solid-state lighting, biosensing, and energy harvesting. In this Perspective, we will summarize recent research trends in the synthesis and applications of 2D semiconductor materials, focusing on three morphological classes: metal chalcogenides, halide perovskites, and transition metal dichalcogenides. Our aim is to describe the role that 2D geometry plays in the optical and electronic properties of these semiconductor nanostructures and to discuss emerging opportunities in their synthesis and applications.

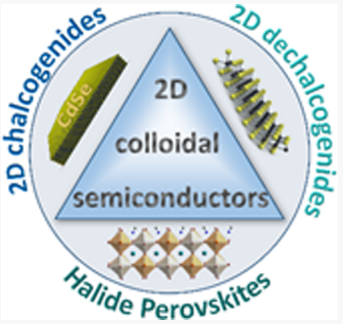

INTRODUCTION

Two-dimensional (2D) colloidal nanomaterials have received a significant amount of attention in recent years. The synergy of the solution-phase processing and 2D quantum confinement has aided the development of novel optoelectronic materials, with a growing number of 2D semiconductors making the list of top-choice materials for electrocatalytic, photovoltaic, and light-emitting applications. The driving force behind the growing interest in 2D semiconductors stems from their appealing quantum properties that differ from those of lower dimensional nanostructures as well as bulk phases. Among the potential benefits, the 2D geometry offers a large surface area, enhanced optical extinction, strong exciton binding, and thickness-tunable band gap. Meanwhile, the solution route to the fabrication and deposition of 2D semiconductors offers a powerful strategy for producing on-demand shapes and sizes, developing heterostructured and intercalated compositions, or processing nanoparticles on substrates.

The family of 2D semiconductors can be subdivided into three basic categories (see Figure 1): (1) graphene-like, single or several-layered structures, including nitrides,[1,2] transition metal dichalcogenides (TMDCs) (e.g., MoS_2), metal oxides,[3] metal−organic frameworks nanosheets (MOFs),[4] covalent−organic frameworks (COFs),[5] MXenes,[6] layered double hydroxides (LDHs),[7] and 2D metals;[8] (2) halide perovskite-derived 2D materials with either a layered hybrid morphology (e.g., Ruddlesden−Popper (RP) type) or a fully inorganic composition; and (3) transition metal chalcogenide (TMC) nanoplatelets (NPLs) and nanoribbons (e.g., CdSe or PbS). In recent years, colloidal routes to the synthesis and deposition of these materials have evolved as an alternative to more traditional methods based on chemical vapor deposition (CVD),[9] molecular beam epitaxy,[10] and mechanical exfoliation,[11] offering superior capabilities in terms of nanoparticle design and substrate processability. In this Perspective, we will briefly review the basic properties and distinctive characteristics of three aforementioned 2D material classes and highlight some of the recent advances and emerging trends associated with each 2D morphology.

DISCUSSION

2D Transition Metal Chalcogenides. The remarkable light-emitting characteristics represent one of the primary reasons for the rising popularity of 2D TMCs. The beneficial effect of the 2D geometry on the optical properties of TMC colloids is illustrated through a side-by-side comparison between 0D and 2D CdSe-based quantum dots (QDs) in Figure 2a. Arguably, the most rewarding feature of the 2D architecture is a narrow emission line width (40−50 meV).[12,13] Compared with 0D CdSe nanocrystals (NCs), the photoluminescence (PL) full width at half-maximum (fwhm) of 2D CdSe NPLs is about half the value, which represents a significant improvement in the color purity for potential applications (Figure 2a). Such narrow PL line widths result from the uniform thickness of 2D CdSe colloids, which are composed of a well-defined number of atomic layers. Small

Received: July 27, 2020
Revised: August 28, 2020
Published: September 3, 2020

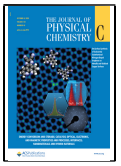

https://dx.doi.org/10.1021/acs.jpcc.0c06868
J. Phys. Chem. C 2020, 124, 21895−21908

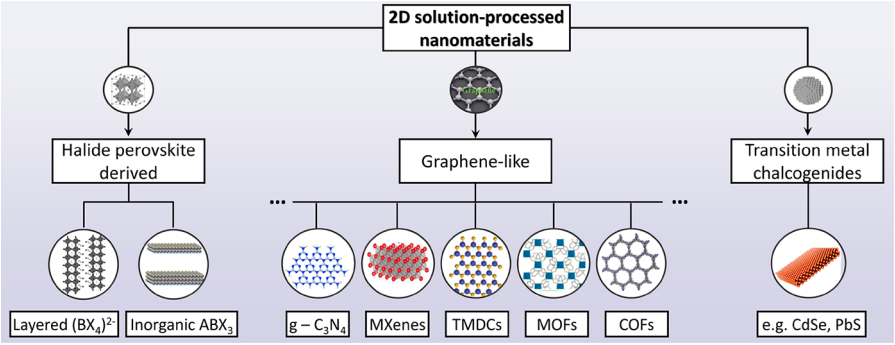

Figure 1. Popular classes of 2D solution-processed semiconductor nanocrystals.

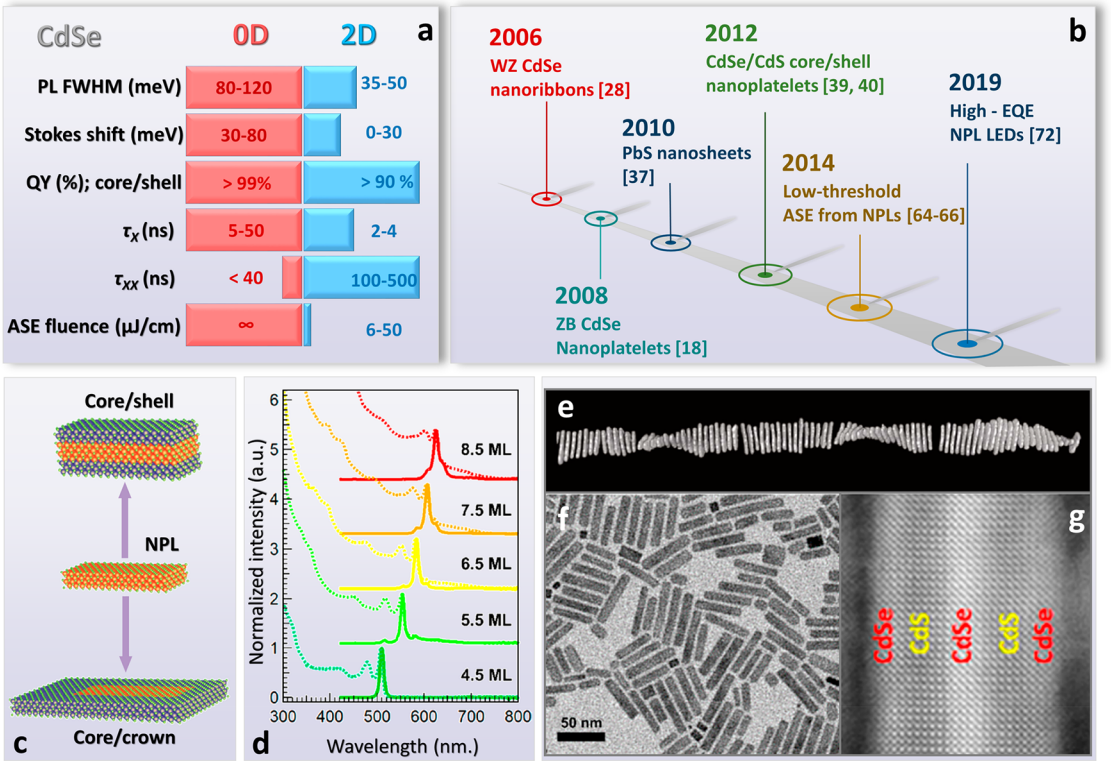

Figure 2. (a) Comparison of optoelectronic properties between 0D and 2D CdSe-based colloids. (b) Chronology of 2D TMC material development highlighting important milestones. (c) Representation of core/shell and core/crown NPL geometries. Adapted with permission from ref 40. Copyright 2012 American Chemical Society. (d) Optical characteristics of CdSe NPLs showcasing narrow emission line widths and a broad range of spectral tunability. Adapted with permission from ref 36. Copyright 2018 American Chemical Society. (e) Tomographic reconstruction of CdSe NPLs self-assembled into twisted ribbons. Adapted with permission from ref 27. Copyright 2017 American Association for the Advancement of Science. (f) TEM of 7.5 monolayer CdSe NPLs. Adapted with permission from ref 36. Copyright 2018 American Chemical Society. (g) High-resolution high-angle annular dark-field scanning transmission electron microscopy (HAADF-STEM) image of the 4CdSe/5CdS/4CdSe/5CdS/4CdSe NPL heterostructure. Adapted with permission from ref 57. Copyright 2019 American Chemical Society.

Stokes shifts are another testament to the uniform thickness of 2D TMC nanostructures. The lack of thickness variations across CdSe NPLs leads to a flat energy landscape, which gives rise to relatively low Stokes shifts of 0−30 meV[14] (as compared with the typical 25−85 meV range reported for 0D CdSe NCs[15]). Finally, 2D CdSe NPLs exhibit a high photoluminescence quantum yield (PLQY) resulting from a low density of exciton and charge traps along the surface[16] as well as strong exciton binding.[17] Even without shelling, it is generally possible to achieve a PLQY in the 20−50% range.[18−21] Meanwhile, the introduction of the wide-gap shell allows the CdSe-based nonresonant photoluminescence (NPL) emission QY to be extended to >90%.[57]

A large density of states (DOS) represents another appealing characteristic of 2D TMC nanostructures. An increased DOS arises from the relaxed confinement in the two lateral dimensions of 2D TMCs, making this geometry the preferred option for light sensitization and biosensing as a high oscillator strength absorber. Owing to the large DOS, 2D CdSe NPLs can also exhibit an enhanced extinction for the intersubband absorption, with corresponding transitions tunable in the infrared range across important telecommunications wavelengths.[22] Further advantages of the 2D geometry are evident in energy transfer applications, where the synergy of a large DOS and a low Stokes shifts contributes to an efficient cascade energy transfer in nanosheet assemblies.[22,23] An increased

https://dx.doi.org/10.1021/acs.jpcc.0c06868
J. Phys. Chem. C 2020, 124, 21895−21908

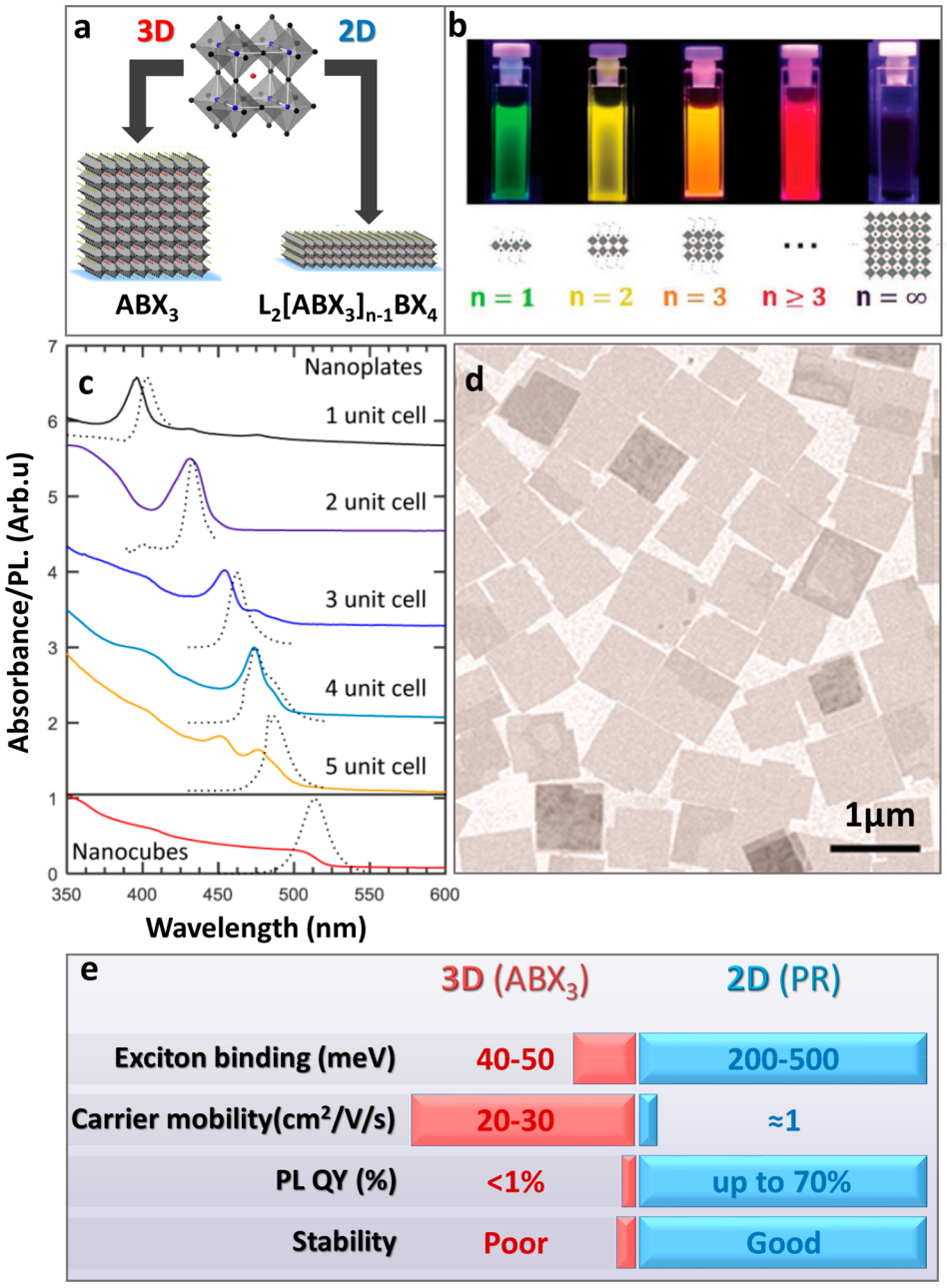

Figure 3. (a) Representation of cubic (3D) and nanosheet (2D) geometries of halide perovskites. A = cesium, formamidinium, methylammonium; B = Pb, Sn; X = Cl, Br, I; L = butylammonium, octylammonium. Adapted with permission from ref 127. Copyright 2017 American Chemical Society. (b) Images of cuvettes containing $MAPbBr_yI_{3-y}$ NPL suspensions illuminated with UV light. From left to right, the thickness increases from a single monolayer (n = 1) stepwise to a bulk-like value (n = ∞). Adapted with permission from ref 115. Copyright 2016 Wiley-VCH. (c) Absorption (solid lines) and emission (dashed lines) spectra of all-inorganic, 2D $CsPbBr_3$ NPLs and 0D $CsPbBr_3$ nanocubes. Adapted with permission from ref 123. Copyright 2016 American Chemical Society. (d) TEM image of 2D $CsPbBr_3$ nanosheets. Adapted with permission from ref 125. Copyright 2016 American Chemical Society. (e) Comparison of optoelectronic properties between bulk 3D (red) and quasi-2D (blue) hybrid halide perovskites.

number of states in 2D semiconductors is also important for multiexciton properties and applications. First, a high degeneracy of band edge excitations in 2D TMCs allows more excitons to be injected within the same particle as compared with lower dimensional colloids.[24] This property is potentially useful for multielectron photocatalytic applications, which require more than a single photoinduced charge to complete a full catalytic cycle (e.g., H_2 production or water oxidation). Second, a large DOS in conjunction with a low electron−hole overlap in 2D TMCs give rise to long-lived multiexciton populations. For instance, the biexciton lifetime of 2D CdSe NPLs exceeds that of 0D CdSe QDs by more than an order of magnitude. (See Figure 2a.) The ability to achieve long-lived biexciton populations in 2D NPLs has been actively explored toward the realization of a low-threshold amplified stimulated emission (ASE) in QD lasing media. Other interesting phenomena associated with the 2D geometry include the possibility of surface-spin-polarized exciton emission[25] and electron shakeup in 2D TMC NPLs.[26]

https://dx.doi.org/10.1021/acs.jpcc.0c06868
J. Phys. Chem. C 2020, 124, 21895−21908

Chronologically, the development of 2D TMCs has commenced with the demonstration of 1.4 nm thick wurtzite CdSe nanosheets, called nanoribbons or quantum belts.[16,28−30] (See Figure 2b.) The synthesis of these nanostructures employed a so-called soft templating approach,[19] which was presumably driven by the oriented attachment of preformed $(CdSe)_{13}$ clusters into stripes. Annealing of these cluster stripes produced 1.4 nm colloidal sheets with an atomically uniform thickness.[16,19,31] Following the demonstration of CdSe nanoribbons, similar protocols were developed for the synthesis of 2D CdS,[32] CdTe,[29] ZnS,[33] and ZnSe[33] colloids. Tunable-thickness, zincblende (ZB) 2D TMCs were first demonstrated by Ithurria in 2008.[18] These nanostructures exhibited more complicated growth dynamics, recently investigated in the work of Norris et al.[34] It was proposed that in the case of ZB NPLs, faster growth occurred on thin facets, which, in comparison with large planar surfaces, had lower activation barriers. A similar approach was subsequently adapted for the fabrication of CdSe nanodisks.[35] With a proper postsynthetic treatment, these strategies have allowed the NPL thickness to be tuned in a broad 1−3 nm range (up to eight monolayers, Figure 2c−f).[36] A comparable method was employed for the synthesis of PbS nanosheets that were formed through the oriented attachment of <3 nm NCs in the presence of chloride compounds.[37]

The synthesis of 2D TMCs progressed over the years, bringing about a broad diversity of morphologies and materials. An important milestone was the demonstration of CdSe/CdS core/shell NPL heterostructures exhibiting PLQYs of up to 80%.[38] (See Figure 2b,c.) The shell growth procedure could be performed with monolayer-level precision through the use of the colloidal atomic layer deposition method (c-ALD),[39,40] which employed self-limiting growth steps. In addition to a regular core/shell CdSe/CdS NPL geometry, a novel heterostructured morphology comprising a CdSe/CdS core/crown arrangement has also been reported (Figure 2c).[41,42] In this case, a CdSe core domain was overgrown by CdS only in lateral dimensions. The resulting CdS crown was shown to efficiently funnel optical excitation into the CdSe core.[42] The crown deposition strategy was subsequently adapted for the synthesis of type-II core/crown NPLs comprising CdSe/CdTe semiconductor combination.[43] Going beyond Cd-based NPLs, 2D colloids of other semiconductors have been synthesized through various strategies. Cation exchange techniques[44] have been employed to convert CdSe/CdS NPLs to Cu_2Se/Cu_2S, PbSe/PbS, and ZnSe/ZnS.[45] Meanwhile, a popular Pb → Cd cation exchange strategy was applied to grow a CdS shell in PbS NPLs, enabling strongly emissive PbS/CdS core/shell NPLs (PLQY = 11%).[46,47] The synthesis of noncadmium 2D TMC colloids, including Cu_2S[48] and SnSe[49] NPLs as well as layered FeS_2[50] and InSe,[51] followed similar hot-injection chemistries. For instance, SnSe[49] NPLs were grown via the coalescence of smaller dots and sheets into larger NPL structures. Mn^{2+} doping further diversified the library of 2D TMC materials, enabling a giant exciton Zeeman splitting.[52,53] It was shown that Mn^{2+} ions could substitute one or two Cd^{2+} ions in $(CdSe)_{13}$ clusters prior to their oriented attachment into nanosheets. Meanwhile, highly luminescent copper-doped ultrathin CdSe NPLs have proven promising as phosphors for white-light generation.[54] In addition, more complex structures,[55,56] such as core/barrier/crown and double-well NPLs (Figure 2g),[57] have recently been synthesized.[58] A more detailed description of the 2D TMC synthetic progress is available in several recent review papers.[59−63]

The unique properties of 2D TMC colloids have been exemplified through the demonstration of high-efficiency optoelectronic devices. Active lasing media represent one of these applications. A combination of long-lived biexcitons and narrow emission line widths in 2D core/shell NPLs has enabled a low pump threshold fluence for ASE in the 4.4−6 $\mu J/cm^2$ range under pulse excitation.[64−66] Narrow emission line widths have also spurred the development of NPL light-emitting diodes (LEDs).[67−69] Although these devices are relatively young,[70] NPL-based LEDs have already reached an impressive external quantum efficiency (EQE) of 19.2%,[71] which is comparable to those of the best QD LEDs[72] and organic light-emitting transistors (OLETs).[73] From the point of view of electronic transport, 2D materials are generally of utmost interest for achieving improved conduction. Nevertheless, a somewhat slower pace has been observed in the development of electron-transport applications, which, thus far, has resulted in the successful demonstration of a prominent photoconductivity response from PbS and CdSe NPLs.[37,74]

2D Halide Perovskites. The first reports of 2D solution-processed halide perovskites date back to 30 years ago.[75−77] It was not until recently, however, that the renewed demand for these materials had risen in the wake of high-efficiency 3D perovskite photovoltaic devices.[78−82] Following the inaugural demonstration of dye-sensitized solar cells,[78] utilizing ABX_3 hybrid perovskite absorbers (A is an organic cation, B is commonly Pb^{2+}, and X is a halide; see Figure 3a), the 2D hybrid morphology gained considerable interest as a quantum-confined version of these materials. Many benefits of quasi-2D[83−86] halide perovskites have been associated with one particular geometry featuring an RP-type, $(L)_2(A)_{n-1}B_nX_{3n+1}$, chemical composition (where $L = RNH_3^+$ = organic spacer; A^+ = Cs, CH_3NH_3; B^{2+} = Pb, Sn, Ge; X^- = Cl, Br, I; see Figure 3a). It employs a quantized number of $(BX_4)^{2-}$ single layers, decoupled from each other by organic chains, which resembles the structure of traditional semiconductor quantum wells. Central to the success of RP perovskites was the possibility of tuning the number of 2D monolayers, which allowed the band gap (Figure 3b) and the flow of the excitation energy in light-emitting or light-harvesting assemblies to be controlled.[87,88] Meanwhile, the presence of a strong 2D quantum confinement in each $(BX_4)^{2-}$ nanosheet has given rise to an enhanced exciton binding energy[89] and improved humidity stability as compared with the 3D ABX_3 counterparts.[84,87]

The ability to assemble quantum-well structures via the solution processing of quasi-2D halide perovskites[90−93] has inspired the development of solar cells,[84,94] LEDs,[95] resistive switching memories,[96] and photodetectors.[97] In the case of light-emitting applications, the quasi-2D morphology provided a unique tool for funneling electrical charges from large-band-gap components (thin layers) into small-band-gap recombination phases (thick layers) for an efficient concentration of energy. Along with the high PLQY (up to 70%)[98] and improved stability, the benefits of the quasi-2D RP perovskites have materialized in LEDs, with electroluminescence quantum efficiency (EQE) of 20.1%,[95,99−102] which nearly matches that of commercialized devices.[103] Similar to LEDs, perovskite solar cells have taken advantage of quasi-2D quantum wells to control the energy flow across 2D layers. Aided by the hot-casting film deposition strategy,[104] the best examples of quasi-2D perovskite solar cells were able to achieve a power

https://dx.doi.org/10.1021/acs.jpcc.0c06868
J. Phys. Chem. C 2020, 124, 21895−21908

conversion efficiency (PCE) of 17.5%.[105] Meanwhile, stacking 2D/3D phases has enabled additional improvements in device performance and stability, leading to PCE of 22%.[106] These characteristics have inspired the development of quasi-2D perovskite photodetectors.[107] With the optimized thickness of $n = 4(BX_4)^{2-}$ layers, quasi-2D hybrid perovskite nanowire photodetectors showed a responsivity of 1.5×10^4 A/W and a detectivity of 7×10^{15} Jones.[97] Remarkably, the latter figure of merit was two orders of magnitude greater than that of commercial silicon photodiodes. It should be noted that most of the aforementioned application examples have relied on solution-phase processing of 2D films. Nevertheless, applications requiring large sheet areas have been known to employ CVD[90,108−110] or exfoliation-based[111] techniques for the direct growth of 2D flakes (e.g., $MAPbI_3$) for utilization in photodetectors.[112] These noncolloidal strategies have been the subject of several recent reviews.[113,114]

All-inorganic, 0D $CsPbX_3$ perovskites were first introduced by Protesescu and Kovalenko et al.[116] in 2015. The key benefit of this morphology was the absence of a volatile organic component, which usually compromised the device stability of quasi-2D hybrid perovskites. The 0D geometry also offered the highest degree of quantum confinement, enabling narrow emission bandwidths (<100 meV), high PLQYs (up to 90−100%), and short radiative lifetimes (1−29 ns).[116] These promising characteristics of 0D $CsPbX_3$ QDs have quickly materialized in the demonstration of all-inorganic perovskite solar cells,[117,118] lasing media,[119,120] and high-efficiency LEDs.[121] Shortly after the demonstration of 0D $CsPbX_3$ QDs, the original synthetic strategy was adapted to fabricating 2D NPLs with monolayer thickness control (Figure 3c,d).[122−133] These 2D $CsPbX_3$ colloids represented the first all-inorganic 2D materials of halide perovskites, offering some interesting optoelectronic characteristics. For instance, the exciton binding energy of 2D NPLs (120−280 meV) was three to five times greater than that of 0D QDs, which implied a greater stability for optoelectronic devices (Figure 3e). Furthermore, the 2D morphology allowed the blue spectral region to be accessed[134] with better overall PLQY than that of 0D counterparts, which has prompted the development of blue LEDs.[135,136] Finally, 2D $CsPbX_3$ were deemed more compatible for large-area devices, such as photodetectors.[137]

2D Transition Metal Dichalcogenides. Starting with the discovery of graphene,[138,139] atomically thin 2D nanomaterials have drawn the vast attention of the scientific community.[140] The promise of novel optoelectronic properties in 2D layered structures has given rise to a vast library of materials, which now include nitrides (h-BN, $g\text{-}C_3N_4$),[1,2] TMDCs (e.g., MoS_2,), layered metal oxides,[3] MOFs,[4] COFs,[5] MXenes,[6] LDHs,[7] and metals[8] (see Figure 1). In this Perspective, we focus on TMDCs as representatives of 2D semiconductors and one of the most studied classes of layered 2D materials given by a generalized formula of MX_2 (e.g., MoS_2, WS_2, $MoSe_2$, WSe_2, and $MoTe_2$; see Figure 4a,b).[141,142] These structures exhibit a number of extraordinary properties, which include a layer-dependent band gap, high activities for hydrogen evolution at unsaturated edge sites,[143] and high theoretical capacity for charge storage (due to a large surface area).[144,145] Furthermore, colloidal 2D TMDCs can be hybridized with graphene and other materials to achieve superior electrochemical and photocatalytic properties.[146−149]

Early strategies for the fabrication of TMDC materials have relied on mechanical/chemical exfoliations and CVD. CVD has been particularly effective for growing high-quality sheets with controllable size and thickness;[153] however, the experimental requirements of high temperature, high vacuum, and specific substrates have inherently limited the feasibility of CVD-grown TMDCs in a number of applications. The colloidal synthesis of 2D TMDCs,[154,155] on the contrary, promises low cost and scalability, which are essential prerequisites for energy storage/conversion applications.[156] Solution-based strategies also provide a rich platform for the chemical functionalization and hybridization of TMDCs with other materials. In recent years, colloidal techniques for the synthesis and processing of 2D TMDCs, including top-down liquid-phase exfoliation methods[154] and bottom-up chemical synthesis,[157−160] have gradually evolved to achieve uniform compositions and sizes as well as to attain particular metastable phases of TMDCs (Figure 4c,d).

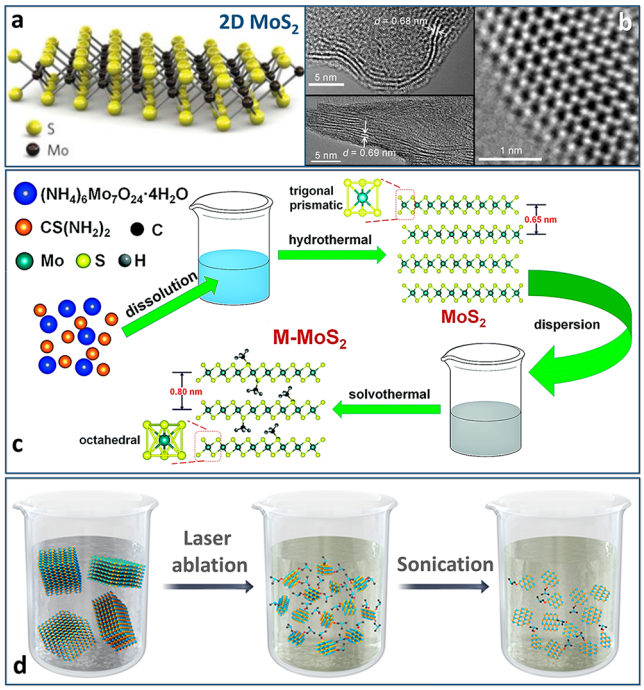

Figure 4. (a) Schematic illustration of a single-layer MoS_2. Adapted with permission from ref 150. Copyright 2011 Springer. (b) High-resolution TEM images of MoS_2 layers. Adapted with permission from ref 157. Copyright 2014 American Chemical Society. (c) Schematic illustration for the solvothermal synthesis of pristine MoS_2 and interlayer-expanded methyl-functionalized (M-MoS_2) nanosheets. Adapted with permission from ref 151. Copyright 2017 The Royal Society of Chemistry. (d) Two-step synthesis of colloidal 2D TMDCs by means of femtosecond laser ablation and sonication-assisted liquid exfoliation. Adapted with permission from ref 152. Copyright 2019 Nature Research.

The advent of colloidal strategies for processing of 2D TMDCs has opened up new opportunities for device applications.[145,161,162] Rechargeable batteries represent one of such examples, where TMDCs offer a high charge storage capacity owing to the large surface area and low intercalation barriers. The main issue of exfoliated TMDC flakes is that they are subject to van der Waals aggregation back into a layered bulk configuration. Colloidal processing can help the avoidance of such limitations by enabling the intercalation of TMDCs with other conductive materials to form composite electrodes.[163] Solution-phase methods have also contributed to electrocatalytic applications of TMDCs, where materials such

https://dx.doi.org/10.1021/acs.jpcc.0c06868
J. Phys. Chem. C 2020, 124, 21895−21908

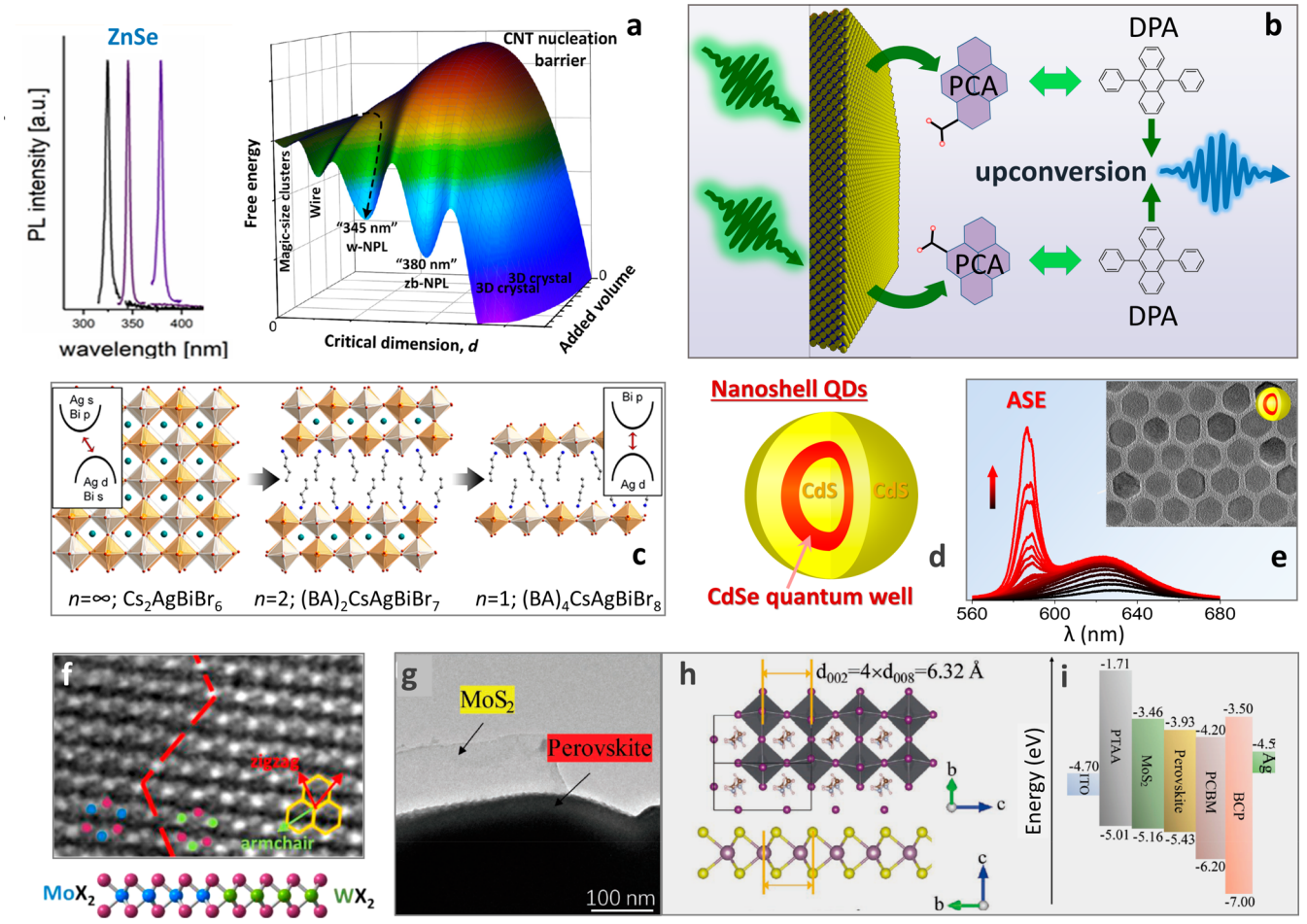

Figure 5. (a) Emission of ZnSe NPLs and the potential energy landscape for the formation of different-dimensionality structures (magic-sized clusters, 1D, 2D, or 3D) with a characteristic evolution of the free energy. An example of the reaction trajectory leading to "345 nm" ZnSe NPLs is shown by the dashed arrow. Adapted with permission from ref 180. Copyright 2020 American Chemical Society. (b) Proposed green-to-blue upconversion in an assembly of CdSe NPLs and (1-pyrenecarboxylic acid (PCA)). Triplet energy transfer from an NPL to a PCA molecule is enhanced by the surface localization of charges and is followed by triple−triplet annihilation in diphenylanthracene (DPA). (c) Layered double perovskites with heavy-metal-free compositions: $(BA)_4AgBiBr_8$ (n = 1; BA = $CH_3(CH_2)_3NH_3^+$) and $(BA)_2CsAgBiBr_7$ (n = 2) and the 3D double perovskite $Cs_2AgBiBr_6$. Adapted with permission from ref 173. Copyright 2018 American Chemical Society. (d) Schematic illustration of a 2D $CdS_{bulk}/CdSe/CdS_{shell}$ quantum-well nanoshell geometry. (e) Amplified stimulated emission from 2D $CdS_{bulk}/CdSe/CdS_{shell}$ QDs observed at a low excitation fluence threshold of 38 $\mu J/cm^2$. (f) High-resolution (HAADF-STEM) image of the heterointerface of the WSe_2−$MoSe_2$ lateral heterostructure. Adapted with permission from ref 174. Copyright 2015 American Chemical Society. (g) Top-view TEM image of MoS_2 with a $MAPbI_3$ perovskite layer grown on its surface. (h) Side view of the atomic crystal heterojunction of $MAPbI_3$ and MoS_2. (i) Energy band structure of the perovskite solar cell with a MoS_2 interlayer. Panels g−i are adapted with permission from ref 175. Copyright 2019 Wiley-VCH.

as MoS_2 show promise as low-cost catalysts for the electron-driven hydrogen-evolution reactions (HERs).[164] As a result of solution processing, MoS_2 could be conjugated with noble-metal NCs, leading to enhanced catalytic performance.[165,166] Similarly, metal oxide catalytic heterostructures were developed by hybridizing TiO_2[167] and Fe_3O_4[168] with MoS_2 nanosheets. More recently, solution methods were used to fabricate TMDC/chalcogenide heterojunctions (e.g., MoS_2/CdS and WS_2/CdS) suitable for photocatalytic H_2 production.[169] In addition to catalytic and battery applications, solution-processed TMDCs have also been employed in biomarkers,[170] sensors,[171] and field-effect transistors.[172]

■ CHALLENGES AND PERSPECTIVES

Solution-processed 2D semiconductors represent a relatively new generation of nanomaterials. Like most quantum-confined structures, 2D materials benefit from a tunable band gap. In addition, the 2D geometry leaves a unique imprint on the optoelectronic characteristics of semiconductor QDs, leading to such attractive features as ultranarrow emission line widths and long-lived biexcitons in TMCs, improved humidity stability and strong exciton binding in 2D halide perovskites, and large reactive surfaces in TMDCs.

Many properties of 2D semiconductor nanostructures originate from surfaces. Notably, the effect of surfactants on both the and structural properties of these materials is uniquely different for the three structural classes investigated in this Perspective. For instance, most Cd-based 2D TMC colloids (e.g., CdSe, CdS NPLs) are structurally static with respect to surface ligand interactions and do not undergo morphological charges upon ligand desorption. As a result, 2D TMCs are stable both in solution and in a solid form under ambient conditions. The main issue of colloidal 2D TMCs concerns the effect of surface ligands on optoelectronic properties. This is because even a partial loss of surfactants in the majority of 0D and 2D TMC nanostructures produces surface states within

https://dx.doi.org/10.1021/acs.jpcc.0c06868
J. Phys. Chem. C 2020, 124, 21895−21908

the nanoparticle band gap. These low-energy states quench optical and electrical excitations in 2D TMC colloids, degrading their performance. Consequently, shelling of 2D TMCs is often required for device applications. In contrast with TMCs, the more dynamic halide perovskite system is easily destabilized by surface chemistry manipulations, leading to halide vacancies or phase transformations. This appears to be the main obstacle for both hybrid and inorganic perovskite devices. Contrary to TMCs, however, the properties of halide perovskites are more defect-tolerant. The dynamic changes in their surface passivation do not always produce low-energy states that quench the PL or trap photoinduced charges. In short, halide perovskites have poor structural stability, but their optoelectronic properties are less affected by the loss of surfactants. Similar to TMCs, TMDCs are structurally stable with respect to ligand interactions. TMDC colloids are also more soluble than TMCs and perovskite nanostructures and generally require lower ligand densities. The main issue of solution-processed TMDCs concerns their electrical performance in solids. Molecular ligands, which are a byproduct of the solution synthesis or processing, inhibit the transfer of charges, presenting significant hurdles for device applications of 2D TMDCs. Consequently, improved protocols for removing surface molecules from chemically prepared TMDCs and TMDC-based heterostructures are in a great demand.

2D Transition Metal Chalcogenides. The future development of 2D TMC materials is likely to explore their attractive PL characteristics. Ultranarrow PL line widths and high QYs of Cd-based chalcogenide NPLs have already materialized in the demonstration of efficient LEDs[71] and will undoubtedly continue to generate research activity in light-emitting materials. Colloidal 2D TMCs are also likely to emerge at the forefront of nanoscale morphologies for QD lasing.[176] This is because 2D TMCs are among the very few nanoscale materials that offer a combination of long multi-exciton lifetimes[177] and low exciton recombination losses, the synergy of which warrants a low-threshold ASE.[178] Finally, one could envision the implementation of 2D core/crown TMC films in luminescent solar concentrators,[42] where high optical extinction and strong exciton binding could lead to a competitive performance.[179]

A smooth transition of the 2D TMC materials to device applications is contingent upon the successful resolution of several synthetic issues. One of those concerns the toxicity of cadmium and other heavy-metal ions, which is likely to cause restricted applications. At the present, NPLs of "green" semiconductors are much less explored. The synthesis of these materials requires a mechanistic understanding of the complex growth reactions associated with 2D TMC phases. A step forward toward addressing this issue was recently made through the realization of Zn-based NPLs exhibiting UV emission (Figure 5a).[180] A novel synthetic approach used in that study may suggest future strategies for the fabrication of non-Cd 2D TMC materials. Synthetic scalability represents another potential issue of 2D TMCs. A typical colloidal synthesis of NPLs yields a high fraction of non-2D structures (e.g., clusters and spherical QDs) that need to be isolated and discarded. Whereas separating heavier NPLs from the reaction byproduct is usually possible, a more directed synthesis of NPLs would prove to be more economical and scalable.

Several future directions for the possible expansion of 2D TMC materials could be expected as a result of emerging research in this field. For instance, photocatalytic systems utilizing 2D NPLs are likely to receive attention due to their large multiphoton absorption cross sections relative to 0D and 1D nanostructures. Because most photochemical reactions require multiple excited electrons (e.g., two-electron H_2 production or four-hole water oxidation),[181,182] a single semiconductor QD must capture a minimum of several photons to complete the photocatalytic cycle. Considering that multiphoton absorption grows proportionally to the particle volume,[183] larger size 2D TMCs should result in enhanced photocatalytic rates.[184,185] These expectations are strongly supported by early reports of an enhanced H_2 production yield in 2D CdS NPLs.[186−188] Future applications of 2D TMCs are also likely to target triplet energy transfer reactions. Recent studies have shown that 0D semiconductor NCs can transfer triplet excitons to a surrounding solid matrix or acceptor dyes[189,190] through a Dexter electron-transfer mechanism. This is a short-range process that benefits from a strong overlap of donor and acceptor wave functions. In this regard, 2D TMCs may represent the preferred geometry of a triplet exciton donor because both excited charges in nanosheets are located on the surface (Figure 5b). Other possibilities for the development of 2D applications could be associated with a relatively new member of the 2D TMC family known as nanoshell QDs[191−193] (Figure 5d,e). These colloids represent a modification of quantum dot quantum wells (QDQWs),[194−196] where the 2D spherical shell of CdSe is grown onto bulk-size CdS seeds, as illustrated in Figure 5d. The presence of a bulk-size core in nanoshell QDs allows the volume of the quantum-confined layer to be increased beyond that of NPLs, which results in a lower exciton density and long multiexciton lifetimes.[191] Furthermore, the thickness of the 2D layer in nanoshell QDs is not limited to six to eight monolayers, as in the case of NPLs, and can offer broader spectral tuning of the emissive shell. Meanwhile, a nearly spherical shape of nanoshells is expected to facilitate their assembly into close-packed solids, a task that is notoriously challenging in the case of 1D or 2D semiconductor colloids.

2D Halide Perovskites. 2D halide perovskites already outperform their 3D counterparts in photovoltaic and light-emitting devices. With reported device performance often matching or surpassing industry standards, the future challenges are likely to focus on ensuring the long-term stability of organometallic halide perovskites in moist environments.[197] A promising route to achieve this goal relies on incorporating graphene or other 2D TMDCs structures in 2D perovskite films, which may offer a feasible solution to the stability issue.[198] Furthermore, interfacing halide perovskites with other 2D materials or carbon nanotubes[199] may allow the realization of new functional materials and devices.[200] We should also mention that many opportunities lie ahead for a relatively new class of all-inorganic 2D perovskites (e.g., $CsPbX_3$ nanosheets). One of the challenges in the future development of these materials concerns the ability to fabricate large-area structures. Stacking layers of different thicknesses represents another important goal that could enable energy funneling in assemblies of 2D inorganic perovskites. Significant progress in this direction was recently achieved by Urban et al.,[201] who demonstrated an assembly of $CsPbBr_3$ NPLs exhibiting cascade FRET, similar to energy funnels in RP perovskite films.

Replacing or substituting lead with nontoxic metal ions will result in more environmentally friendly compounds with new properties and functionalities. Lead-free perovskites such as

https://dx.doi.org/10.1021/acs.jpcc.0c06868
J. Phys. Chem. C 2020, 124, 21895−21908

$ASnX_3$, $Cs_2AgBiBr_6$, and $A_3M_2X_9$ (M = Bi or Sb) have been identified as promising semiconductors with low toxicity.[202] Another notable example is double perovskite crystals (e.g., $Cs_2AgBiBr_6$ and $Cs_2AgInCl_6$; see Figure 5c).[173,203] Reducing the dimensionality of such 3D double perovskites to 2D will open up new space to explore their optical and electronic properties.

2D Transition Metal Dichalcogenides. The colloidal synthesis of TMDC materials provides a straightforward strategy for the scalable production functionalization and hybridization of nanosheets, thus facilitating their exploration for various applications. A number of colloidal methods have been developed for the preparation of 2D TMDC nanosheets, including solvent-phase exfoliation, surfactant-assisted exfoliation, ion intercalation and exfoliation, and wet chemical methods. After their transfer to a solution, 2D TMDC nanosheets offer great opportunities for the preparation of functional hybrid heteronanostructures with a variety of nanoscale partners, including biomaterials, MOFs, metals, metal oxides, and metal chalcogenides. Presently, the development of colloidal routes to process 2D TMDCs faces a few obstacles, one of which is related to the change in the TMDC surface energy. This interaction is particularly significant in the case of atomically thin layers. Careful analysis of TMDC−ligand systems has to be performed, as many characteristics of the 2D geometry could be suppressed due to ligands. Consequently, the future development of colloidal TMDCs will likely focus on controlling the aforementioned ligand−sheet interactions. As an alternative strategy, effective ligand stripping techniques could be employed for the treatment of deposited or assembled nanosheets.

Synthetic efforts for the development of colloidal TMDCs are likely to focus on two main aspects. The first one is the structure-engineering task, which will focus on the morphological optimization of these materials toward increasing the number of active sites and improving the edge morphology. The other goal is likely to focus on achieving an efficient charge transfer across TMDC materials by means of elemental doping, strain/interface engineering, and 2D heterostructure assembly (Figure 5f−i). The two synthetic efforts will ultimately create a next-generation material platform for achieving novel physical and chemical properties. Future synthetic efforts are also likely to focus on solution-based methods for the preparation of 2D lateral and vertical epitaxial heterostructures,[204,205] providing new opportunities for device applications.[205] The general goal of the colloidal synthesis should also focus on the product scalability. Currently, the amount of colloidal 2D TMDC nanosheets, especially the single-layer TMDC nanosheets, is still relatively low for practical applications in supercapacitors and batteries. Therefore, the high-yield production of a single-layer 2D TMDC is in high demand. Ultimately, solution-phase methods will provide a viable path toward the scalable production, functionalization, and hybridization of TMDC nanosheets, thus facilitating the exploration of TMDC-based nanomaterials.

In summary, 2D semiconductors exhibit unique optoelectronic properties enabled by a relaxed motion of electrical charges along two spatial dimensions. Owing to recent advances in the colloidal synthesis and solution-processing of these materials, the stage is set for the low-cost and scalable production of high-performance light-emitting, charge-transport, and light-harvesting devices. This work summarizes recent research trends in 2D solution-processed semiconductor materials by focusing on three morphological classes: metal chalcogenides, halide perovskites, and TMDCs. We have described the unique role of 2D geometry in the optical and electronic properties of these semiconductor nanostructures and discussed emerging opportunities in their synthesis and applications.

AUTHOR INFORMATION

Corresponding Author

Mikhail Zamkov − *The Center for Photochemical Sciences and Department of Physics, Bowling Green State University, Bowling Green, Ohio 43402, United States;* orcid.org/0000-0002-8638-2972; Email: zamkovm@bgsu.edu

Author

Dmitry Porotnikov − *The Center for Photochemical Sciences and Department of Physics, Bowling Green State University, Bowling Green, Ohio 43402, United States*

Complete contact information is available at: https://pubs.acs.org/10.1021/acs.jpcc.0c06868

Notes

The authors declare no competing financial interest.

Biographies

Prof. Mikhail Zamkov obtained his Ph.D. degrees from Kansas State University in 2003. He is now an Full Professor at Bowling Green State University. His research focuses on the electronic, chemical, and optical properties of semiconductor nanostructures (QDs) and hybrid nanoscale materials prepared by means of colloidal synthesis. Web: http://physics.bgsu.edu/~zamkovm/.

Dmitry Porotnikov is a Ph.D. candidate in Photochemical Science at Bowling Green State University. He obtained his M.S. degree in Material Chemistry in 2017 at Saint-Petersburg State University, Russia. He works under the supervision of Prof. Zamkov at Bowling Green State University. His research is focused on the synthesis and application of colloidal semiconductor nanocrystals.

ACKNOWLEDGMENTS

This work was supported by the Award DE-SC0016872 (M.Z.) funded by the U.S. Department of Energy, Office of Science. D.P. was supported in part by NSF Award DMR-1710063.

REFERENCES

(1) Weng, Q.; Wang, X.; Wang, X.; Bando, Y.; Golberg, D. Functionalized hexagonal boron nitride nanomaterials: emerging properties and applications. *Chem. Soc. Rev.* **2016**, *45*, 3989−4012.

(2) Tan, C.; Zhang, H. Two-dimensional transition metal dichalcogenide nanosheet-based composites. *Chem. Soc. Rev.* **2015**, *44*, 2713−2731.

(3) Ma, R.; Sasaki, T. Two-Dimensional Oxide and Hydroxide Nanosheets: Controllable High-Quality Exfoliation, Molecular Assembly, and Exploration of Functionality. *Acc. Chem. Res.* **2015**, *48*, 136−143.

(4) Peng, Y.; Li, Y.; Ban, Y.; Jin, H.; Jiao, W.; Liu, X.; Yang, W. Metal-organic framework nanosheets as building blocks for molecular sieving membranes. *Science* **2014**, *346*, 1356−1359.

(5) Colson, J. W.; Woll, A. R.; Mukherjee, A.; Levendorf, M. P.; Spitler, E. L.; Shields, V. B.; Spencer, M. G.; Park, J.; Dichtel, W. R. Oriented 2D Covalent Organic Framework Thin Films on Single-Layer Graphene. *Science* **2011**, *332*, 228−231.

(6) Anasori, B.; Lukatskaya, M. R.; Gogotsi, Y. 2D metal carbides and nitrides (MXenes) for energy storage. *Nat. Rev. Mater.* **2017**, *2*, 16098.
(7) Wang, Q.; O'Hare, D. Recent Advances in the Synthesis and Application of Layered Double Hydroxide (LDH) Nanosheets. *Chem. Rev.* **2012**, *112*, 4124−4155.
(8) Han, N.; Wang, Y.; Yang, H.; Deng, J.; Wu, J.; Li, Y.; Li, Y. Ultrathin bismuth nanosheets from in situ topotactic transformation for selective electrocatalytic CO_2 reduction to formate. *Nat. Commun.* **2018**, *9*, 1320.
(9) Zhang, Y.; Zhang, L.; Zhou, C. Review of Chemical Vapor Deposition of Graphene and Related Applications. *Acc. Chem. Res.* **2013**, *46*, 2329−2339.
(10) Poh, S. M.; Zhao, X.; Tan, S. J. R.; Fu, D.; Fei, W.; Chu, L.; Jiadong, D.; Zhou, W.; Pennycook, S. J.; Castro Neto, A. H.; Loh, K. P. Molecular Beam Epitaxy of Highly Crystalline $MoSe_2$ on Hexagonal Boron Nitride. *ACS Nano* **2018**, *12*, 7562−7570.
(11) Novoselov, K. S.; Geim, A. K.; Morozov, S. V.; Jiang, D.; Zhang, Y.; Dubonos, S. V.; Grigorieva, I. V.; Firsov, A. A. Electric Field Effect in Atomically Thin Carbon Films. *Science* **2004**, *306*, 666−669.
(12) Tessier, M. D.; Javaux, C.; Maksimovic, I.; Loriette, V.; Dubertret, B. Spectroscopy of Single CdSe Nanoplatelets. *ACS Nano* **2012**, *6*, 6751−6758.
(13) Pedetti, S.; Nadal, B.; Lhuillier, E.; Mahler, B.; Bouet, C.; Abécassis, B.; Xu, X.; Dubertret, B. Optimized Synthesis of CdTe Nanoplatelets and Photoresponse of CdTe Nanoplatelets Films. *Chem. Mater.* **2013**, *25*, 2455−2462.
(14) Ji, B.; Rabani, E.; Efros, A. L.; Vaxenburg, R.; Ashkenazi, O.; Azulay, D.; Banin, U.; Millo, O. Dielectric Confinement and Excitonic Effects in Two-Dimensional Nanoplatelets. *ACS Nano* **2020**, *14*, 8257−8265.
(15) Qu, L.; Peng, X. Control of Photoluminescence Properties of CdSe Nanocrystals in Growth. *J. Am. Chem. Soc.* **2002**, *124*, 2049−2055.
(16) Liu, Y.-H.; Wayman, V. L.; Gibbons, P. C.; Loomis, R. A.; Buhro, W. E. Origin of High Photoluminescence Efficiencies in CdSe Quantum Belts. *Nano Lett.* **2010**, *10*, 352−357.
(17) Benchamekh, R.; Gippius, N. A.; Even, J.; Nestoklon, M. O.; Jancu, J.-M.; Ithurria, S.; Dubertret, B.; Efros, A. L.; Voisin, P. Tight-binding calculations of image-charge effects in colloidal nanoscale platelets of CdSe. *Phys. Rev. B: Condens. Matter Mater. Phys.* **2014**, *89*, 035307.
(18) Ithurria, S.; Dubertret, B. Quasi 2D Colloidal CdSe Platelets with Thicknesses Controlled at the Atomic Level. *J. Am. Chem. Soc.* **2008**, *130*, 16504−16505.
(19) Liu, Y.-H.; Wang, F.; Wang, Y.; Gibbons, P. C.; Buhro, W. E. Lamellar Assembly of Cadmium Selenide Nanoclusters into Quantum Belts. *J. Am. Chem. Soc.* **2011**, *133*, 17005−17013.
(20) Ithurria, S.; Tessier, M. D.; Mahler, B.; Lobo, R. P. S. M.; Dubertret, B.; Efros, A. L. Colloidal nanoplatelets with two-dimensional electronic structure. *Nat. Mater.* **2011**, *10*, 936−941.
(21) Singh, S.; Tomar, R.; ten Brinck, S.; De Roo, J.; Geiregat, P.; Martins, J. C.; Infante, I.; Hens, Z. Colloidal CdSe Nanoplatelets, A Model for Surface Chemistry/Optoelectronic Property Relations in Semiconductor Nanocrystals. *J. Am. Chem. Soc.* **2018**, *140*, 13292−13300.
(22) Diroll, B. T.; Chen, M.; Coropceanu, I.; Williams, K. R.; Talapin, D. V.; Guyot-Sionnest, P.; Schaller, R. D. Polarized near-infrared intersubband absorptions in CdSe colloidal quantum wells. *Nat. Commun.* **2019**, *10*, 4511.
(23) Rowland, C. E.; Fedin, I.; Zhang, H.; Gray, S. K.; Govorov, A. O.; Talapin, D. V.; Schaller, R. D. Picosecond energy transfer and multiexciton transfer outpaces Auger recombination in binary CdSe nanoplatelet solids. *Nat. Mater.* **2015**, *14*, 484−489.
(24) Scott, R.; Achtstein, A. W.; Prudnikau, A.; Antanovich, A.; Christodoulou, S.; Moreels, I.; Artemyev, M.; Woggon, U. Two Photon Absorption in II−VI Semiconductors: The Influence of Dimensionality and Size. *Nano Lett.* **2015**, *15*, 4985−4992.
(25) Shornikova, E. V.; Golovatenko, A. A.; Yakovlev, D. R.; Rodina, A. V.; Biadala, L.; Qiang, G.; Kuntzmann, A.; Nasilowski, M.; Dubertret, B.; Polovitsyn, A.; Moreels, I.; Bayer, M. Surface spin magnetism controls the polarized exciton emission from CdSe nanoplatelets. *Nat. Nanotechnol.* **2020**, *15*, 277−282.
(26) Antolinez, F. V.; Rabouw, F. T.; Rossinelli, A. A.; Cui, J.; Norris, D. J. Observation of Electron Shakeup in CdSe/CdS Core/Shell Nanoplatelets. *Nano Lett.* **2019**, *19*, 8495−8502.
(27) Jana, S.; de Frutos, M.; Davidson, P.; Abécassis, B. Ligand-induced twisting of nanoplatelets and their self-assembly into chiral ribbons. *Sci. Adv.* **2017**, *3*, e1701483.
(28) Joo, J.; Son, J. S.; Kwon, S. G.; Yu, J. H.; Hyeon, T. Low-Temperature Solution-Phase Synthesis of Quantum Well Structured CdSe Nanoribbons. *J. Am. Chem. Soc.* **2006**, *128*, 5632−5633.
(29) Son, J. S.; Wen, X.-D.; Joo, J.; Chae, J.; Baek, S.-il; Park, K.; Kim, J. H.; An, K.; Yu, J. H.; Kwon, S. G.; Choi, S.-H.; Wang, Z.; Kim, Y.-W.; Kuk, Y.; Hoffmann, R.; Hyeon, T. Angew. Large-Scale Soft Colloidal Template Synthesis of 1.4 nm Thick CdSe Nanosheets. *Angew. Chem., Int. Ed.* **2009**, *48*, 6861−6864.
(30) Pradhan, N.; Xu, H.; Peng, X. Colloidal CdSe Quantum Wires by Oriented Attachment. *Nano Lett.* **2006**, *6*, 720−724.
(31) Wang, Y.; Zhou, Y.; Zhang, Y.; Buhro, W. E. Magic-Size II−VI Nanoclusters as Synthons for Flat Colloidal Nanocrystals. *Inorg. Chem.* **2015**, *54*, 1165−1177.
(32) Son, J. S.; Park, K.; Kwon, S. G.; Yang, J.; Choi, M. K.; Kim, J.; Yu, J. H.; Joo, J.; Hyeon, T. Dimension-Controlled Synthesis of CdS Nanocrystals: From 0D Quantum Dots to 2D Nanoplates. *Small* **2012**, *8*, 2394−2402.
(33) Park, H.; Chung, H.; Kim, W. Synthesis of ultrathin wurtzite ZnSe nanosheets. *Mater. Lett.* **2013**, *99*, 172−175.
(34) Riedinger, A.; Ott, F. D.; Mule, A.; Mazzotti, S.; Knüsel, P. N.; Kress, S. J. P.; Prins, F.; Erwin, S. C.; Norris, D. J. An intrinsic growth instability in isotropic materials leads to quasi-two-dimensional nanoplatelets. *Nat. Mater.* **2017**, *16*, 743−748.
(35) Li, Z.; Peng, X. Size/Shape-Controlled Synthesis of Colloidal CdSe Quantum Disks: Ligand and Temperature Effects. *J. Am. Chem. Soc.* **2011**, *133*, 6578−6586.
(36) Christodoulou, S.; Climente, J. I.; Planelles, J.; Brescia, R.; Prato, M.; Martín-García, B.; Khan, A. H.; Moreels, I. Chloride-Induced Thickness Control in CdSe Nanoplatelets. *Nano Lett.* **2018**, *18*, 6248−6254.
(37) Schliehe, C.; Juarez, B. H.; Pelletier, M.; Jander, S.; Greshnykh, D.; Nagel, M.; Meyer, A.; Foerster, S.; Kornowski, A.; Klinke, C.; Weller, H. Ultrathin PbS Sheets by Two-Dimensional Oriented Attachment. *Science* **2010**, *329*, 550−553.
(38) Tessier, M. D.; Mahler, B.; Nadal, B.; Heuclin, H.; Pedetti, S.; Dubertret, S. Spectroscopy of Colloidal Semiconductor Core/Shell Nanoplatelets with High Quantum Yield. *Nano Lett.* **2013**, *13*, 3321−3328.
(39) Ithurria, S.; Talapin, D. V. Colloidal Atomic Layer Deposition (c-ALD) using Self-Limiting Reactions at Nanocrystal Surface Coupled to Phase Transfer between Polar and Nonpolar Media. *J. Am. Chem. Soc.* **2012**, *134*, 18585−18590.
(40) Mahler, B.; Nadal, B.; Bouet, C.; Patriarche, G.; Dubertret, B. Core/Shell Colloidal Semiconductor Nanoplatelets. *J. Am. Chem. Soc.* **2012**, *134*, 18591−18598.
(41) Prudnikau, A.; Chuvilin, A.; Artemyev, M. CdSe−CdS Nanoheteroplatelets with Efficient Photoexcitation of Central CdSe Region through Epitaxially Grown CdS Wings. *J. Am. Chem. Soc.* **2013**, *135*, 14476−14479.
(42) Tessier, M. D.; Spinicelli, P.; Dupont, D.; Patriarche, G.; Ithurria, S.; Dubertret, B. Efficient Exciton Concentrators Built from Colloidal Core/Crown CdSe/CdS Semiconductor Nanoplatelets. *Nano Lett.* **2014**, *14*, 207−213.
(43) Pedetti, S.; Ithurria, S.; Heuclin, H.; Patriarche, G.; Dubertret, B. Type-II CdSe/CdTe Core/Crown Semiconductor Nanoplatelets. *J. Am. Chem. Soc.* **2014**, *136*, 16430−16438.

https://dx.doi.org/10.1021/acs.jpcc.0c06868
J. Phys. Chem. C 2020, 124, 21895−21908

(44) Son, D. H.; Hughes, S. M.; Yin, Y.; Alivisatos, A. P. Cation Exchange Reactions in Ionic Nanocrystals. *Science* **2004**, *306*, 1009−1012.
(45) Bouet, C.; Laufer, D.; Mahler, B.; Nadal, B.; Heuclin, H.; Pedetti, S.; Patriarche, G.; Dubertret, B. *Chem. Mater.* **2014**, *26*, 3002−3008.
(46) Zhang, H.; Savitzky, B. H.; Yang, J.; Newman, J. T.; Perez, K. A.; Hyun, B.-R.; Kourkoutis, L. F.; Hanrath, T.; Wise, F. W. Colloidal Synthesis of PbS and PbS/CdS Nanosheets Using Acetate-Free Precursors. *Chem. Mater.* **2016**, *28*, 127−134.
(47) Khan, S.; Jiang, Z.; Premathilka, S. M.; Antu, A.; Hu, J.; Voevodin, A. A.; Roland, P. J.; Ellingson, R. J.; Sun, L. Few-Atom-Thick Colloidal PbS/CdS Core/Shell Nanosheets. *Chem. Mater.* **2016**, *28*, 5342−5346.
(48) Zhuang, Z.; Peng, Q.; Zhang, B.; Li, Y. Controllable Synthesis of Cu_2S Nanocrystals and Their Assembly into a Superlattice. *J. Am. Chem. Soc.* **2008**, *130*, 10482−10483.
(49) Vaughn, D. D.; In, S.-I.; Schaak, R. E. A Precursor-Limited Nanoparticle Coalescence Pathway for Tuning the Thickness of Laterally-Uniform Colloidal Nanosheets: The Case of SnSe. *ACS Nano* **2011**, *5*, 8852−8860.
(50) Kirkeminde, A.; Ruzicka, B. A.; Wang, R.; Puna, S.; Zhao, H.; Ren, S. Synthesis and Optoelectronic Properties of Two-Dimensional FeS_2 Nanoplates. *ACS Appl. Mater. Interfaces* **2012**, *4*, 1174−1177.
(51) Lauth, J.; Gorris, F. E. S.; Samadi Khoshkhoo, M.; Chasse, T.; Friedrich, W.; Lebedeva, V.; Meyer, A.; Klinke, C.; Kornowski, A.; Scheele, M.; Weller, H. Solution-Processed Two-Dimensional Ultrathin InSe Nanosheets. *Chem. Mater.* **2016**, *28*, 1728−1736.
(52) Yu, J. H.; Liu, X.; Kweon, K. E.; Joo, J.; Park, J.; Ko, K.-T.; Lee, D. W.; Shen, S.; Tivakornsasithorn, K.; Son, J. S.; Park, J.-H.; Kim, Y.-W.; Hwang, G. S.; Dobrowolska, M.; Furdyna, J. K.; Hyeon, T. Giant Zeeman splitting in nucleation-controlled doped CdSe:Mn^{2+} quantum nanoribbons. *Nat. Mater.* **2010**, *9*, 47−53.
(53) Wang, Y.; Zhang, Y.; Wang, F.; Giblin, D. E.; Hoy, J.; Rohrs, H. W.; Loomis, R. A.; Buhro, W. E. The Magic-Size Nanocluster $(CdSe)_{34}$ as a Low-Temperature Nucleant for Cadmium Selenide Nanocrystals; Room-Temperature Growth of Crystalline Quantum Platelets. *Chem. Mater.* **2014**, *26*, 2233−2243.
(54) Saidzhonov, B. M.; Zaytsev, V. B.; Berekchiian, M. V.; Vasiliev, R. B. Highly luminescent copper-doped ultrathin CdSe nanoplatelets for white-light generation. *J. Lumin.* **2020**, *222*, 117134.
(55) Sun, H.; Buhro, W. E. Core−Shell Cadmium Telluride Quantum Platelets with Absorptions Spanning the Visible Spectrum. *ACS Nano* **2019**, *13*, 6982−6991.
(56) Altintas, Y.; Quliyeva, U.; Gungor, K.; Erdem, O.; Kelestemur, Y.; Mutlugun, E.; Kovalenko, M. V.; Demir, H. V. Highly Stable, Near-Unity Efficiency Atomically Flat Semiconductor Nanocrystals of CdSe/ZnS Hetero-Nanoplatelets Enabled by ZnS-Shell Hot-Injection Growth. *Small* **2019**, *15*, 1804854.
(57) Hazarika, A.; Fedin, I.; Hong, L.; Guo, G.; Srivastava, V.; Cho, W.; Coropceanu, I.; Portner, J.; Diroll, B. T.; Philbin, J. P.; Rabani, E.; Klie, R.; Talapin, D. V. Colloidal Atomic Layer Deposition with Stationary Reactant Phases Enables Precise Synthesis of "Digital" II−VI Nano-heterostructures with Exquisite Control of Confinement and Strain. *J. Am. Chem. Soc.* **2019**, *141*, 13487−13496.
(58) Khan, A. H.; Bertrand, G. H. V.; Teitelboim, A.; Sekhar M., C.; Polovitsyn, A.; Brescia, R.; Planelles, J.; Climente, J. I.; Oron, D.; Moreels, I. CdSe/CdS/CdTe Core/Barrier/Crown Nanoplatelets: Synthesis, Optoelectronic Properties, and Multiphoton Fluorescence Upconversion. *ACS Nano* **2020**, *14*, 4206−4215.
(59) Lhuillier, E.; Pedetti, S.; Ithurria, S.; Nadal, B.; Heuclin, H.; Dubertret, B. Two-Dimensional Colloidal Metal Chalcogenides Semiconductors: Synthesis, Spectroscopy, and Applications. *Acc. Chem. Res.* **2015**, *48*, 22−30.
(60) Bouet, C.; Tessier, M. D.; Ithurria, S.; Mahler, B.; Nadal, B.; Dubertret, B. Flat Colloidal Semiconductor Nanoplatelets. *Chem. Mater.* **2013**, *25*, 1262−1271.
(61) Yang, J.; Son, J. S.; Yu, J. H.; Joo, J.; Hyeon, T. Advances in the Colloidal Synthesis of Two-Dimensional Semiconductor Nanoribbons. *Chem. Mater.* **2013**, *25*, 1190−1198.
(62) Wang, F.; Wang, Y.; Liu, Y.-H.; Morrison, P. J.; Loomis, R. A.; Buhro, W. E. Two-Dimensional Semiconductor Nanocrystals: Properties, Templated Formation, and Magic-Size Nanocluster Intermediates. *Acc. Chem. Res.* **2015**, *48*, 13−21.
(63) Nasilowski, M.; Mahler, B.; Lhuillier, E.; Ithurria, S.; Dubertret, B. Two-Dimensional Colloidal Nanocrystals. *Chem. Rev.* **2016**, *116*, 10934−10982.
(64) Grim, J. Q.; Christodoulou, S.; Di Stasio, F.; Krahne, R.; Cingolani, R.; Manna, L.; Moreels, I. Continuous-wave biexciton lasing at room temperature using solution-processed quantum wells. *Nat. Nanotechnol.* **2014**, *9*, 891−895.
(65) She, C.; Fedin, I.; Dolzhnikov, D. S.; Demortière, A.; Schaller, R. D.; Pelton, M.; Talapin, D. V. Low-Threshold Stimulated Emission Using Colloidal Quantum Wells. *Nano Lett.* **2014**, *14*, 2772−2777.
(66) Zhang, L.; Yang, H.; Yu, B.; Tang, Y.; Zhang, C.; Wang, X.; Xiao, M.; Cui, Y.; Zhang, J. Low-Threshold Amplified Spontaneous Emission and Lasing from Thick-Shell CdSe/CdS Core/Shell Nanoplatelets Enabled by High-Temperature Growth. *Adv. Opt. Mater.* **2020**, *8*, 1901615.
(67) Xiao, P.; Huang, J.; Yan, D.; Luo, D.; Yuan, J.; Liu, B.; Liang, D. Emergence of Nanoplatelet Light-Emitting Diodes. *Materials* **2018**, *11*, 1376.
(68) Zhang, F.; Wang, S.; Wang, L.; Lin, Q.; Shen, H.; Cao, W.; Yang, C.; Wang, H.; Yu, L.; Du, Z.; Xue, J.; Li, L. S. Super color purity green quantum dot light-emitting diodes fabricated by using CdSe/CdS nanoplatelets. *Nanoscale* **2016**, *8*, 12182−12188.
(69) Giovanella, U.; Pasini, M.; Lorenzon, M.; Galeotti, F.; Lucchi, C.; Meinardi, F.; Luzzati, S.; Dubertret, B.; Brovelli, S. Efficient Solution-Processed Nanoplatelet-Based Light-Emitting Diodes with High Operational Stability in Air. *Nano Lett.* **2018**, *18*, 3441−3448.
(70) Chen, Z.; Nadal, B.; Mahler, B.; Aubin, H.; Dubertret, B. Quasi-2D Colloidal Semiconductor Nanoplatelets for Narrow Electroluminescence. *Adv. Funct. Mater.* **2014**, *24*, 295−302.
(71) Liu, B.; Altintas, Y.; Wang, L.; Shendre, S.; Sharma, M.; Sun, H.; Mutlugun, E.; Demir, H. V. Record High External Quantum Efficiency of 19.2% Achieved in Light-Emitting Diodes of Colloidal Quantum Wells Enabled by Hot-Injection Shell Growth. *Adv. Mater.* **2020**, *32*, 1905824.
(72) Dai, X.; Zhang, Z.; Jin, Y.; Niu, Y.; Cao, H.; Liang, X.; Chen, L.; Wang, J.; Peng, X. Solution-processed, high-performance light-emitting diodes based on quantum dots. *Nature* **2014**, *515*, 96−99.
(73) Yang, X.; Zhou, G.; Wong, W.-Y. Functionalization of phosphorescent emitters and their host materials by main-group elements for phosphorescent organic light-emitting devices. *Chem. Soc. Rev.* **2015**, *44*, 8484−8575.
(74) Lhuillier, E.; Pedetti, S.; Ithurria, S.; Heuclin, H.; Nadal, B.; Robin, A.; Patriarche, G.; Lequeux, N.; Dubertret, B. Electrolyte-Gated Field Effect Transistor to Probe the Surface Defects and Morphology in Films of Thick CdSe Colloidal Nanoplatelets. *ACS Nano* **2014**, *8*, 3813−3820.
(75) Ishihara, T.; Takahashi, J.; Goto, T. Exciton state in two-dimensional perovskite semiconductor $(C_{10}H_{21}NH_3)_2PbI_4$. *Solid State Commun.* **1989**, *69*, 933−936.
(76) Calabrese, J.; Jones, N. L.; Harlow, R. L.; Herron, N.; Thorn, D. L.; Wang, Y. Preparation and characterization of layered lead halide compounds. *J. Am. Chem. Soc.* **1991**, *113*, 2328−2330.
(77) Mitzi, D. B.; Wang, S.; Feild, C. A.; Chess, C. A.; Guloy, A. M. Conducting Layered Organic-inorganic Halides Containing < 110>-Oriented Perovskite Sheets. *Science* **1995**, *267*, 1473−1476.
(78) Kojima, A.; Teshima, K.; Shirai, Y.; Miyasaka, T. Organometal Halide Perovskites as Visible-Light Sensitizers for Photovoltaic Cells. *J. Am. Chem. Soc.* **2009**, *131*, 6050−6051.
(79) Lee, M. M.; Teuscher, J.; Miyasaka, T.; Murakami, T. N.; Snaith, H. J. Efficient Hybrid Solar Cells Based on Meso-Superstructured Organometal Halide Perovskites. *Science* **2012**, *338*, 643−647.

https://dx.doi.org/10.1021/acs.jpcc.0c06868
J. Phys. Chem. C 2020, 124, 21895−21908

(80) Xing, G.; Mathews, N.; Sun, S.; Lim, S. S.; Lam, Y. M.; Grätzel, M.; Mhaisalkar, S.; Sum, T. C. Long-Range Balanced Electron- and Hole-Transport Lengths in Organic-Inorganic $CH_3NH_3PbI_3$. *Science* **2013**, *342*, 344−347.
(81) Snaith, H. J. Present status and future prospects of perovskite photovoltaics. *Nat. Mater.* **2018**, *17*, 372−376.
(82) Green, M. A.; Ho-Baillie, A.; Snaith, H. J. The emergence of perovskite solar cells. *Nat. Photonics* **2014**, *8*, 506−514.
(83) Borriello, I.; Cantele, G.; Ninno, D. *Ab initio* investigation of hybrid organic-inorganic perovskites based on tin halides. *Phys. Rev. B: Condens. Matter Mater. Phys.* **2008**, *77*, 235214.
(84) Tsai, H.; Nie, W.; Blancon, J.-C.; Stoumpos, C. C.; Asadpour, R.; Harutyunyan, B.; Neukirch, A. J.; Verduzco, R.; Crochet, J. J.; Tretiak, S.; Pedesseau, L.; Even, J.; Alam, M. A.; Gupta, G.; Lou, J.; Ajayan, P. M.; Bedzyk, M. J.; Kanatzidis, M. G.; Mohite, A. D. High-efficiency two-dimensional Ruddlesden−Popper perovskite solar cells. *Nature* **2016**, *536*, 312−316.
(85) Blancon, J.-C.; Tsai, H.; Nie, W.; Stoumpos, C. C.; Pedesseau, L.; Katan, C.; Kepenekian, M.; Soe, C. M. M.; Appavoo, K.; Sfeir, M. Y.; Tretiak, S.; Ajayan, P. M.; Kanatzidis, M. G.; Even, J.; Crochet, J. J.; Mohite, A. D. Extremely efficient internal exciton dissociation through edge states in layered 2D perovskites. *Science* **2017**, *355*, 1288−1292.
(86) Kim, H.; Huynh, K. A.; Kim, S. Y.; Le, Q. V.; Jang, H. W. 2D and Quasi-2D Halide Perovskites: Applications and Progress. *Phys. Status Solidi RRL* **2020**, *14*, 1900435.
(87) Cao, D. H.; Stoumpos, C. C.; Farha, O. K.; Hupp, J. T.; Kanatzidis, M. G. 2D Homologous Perovskites as Light-Absorbing Materials for Solar Cell Applications. *J. Am. Chem. Soc.* **2015**, *137*, 7843−7850.
(88) Smith, I. C.; Hoke, E. T.; Solis-Ibarra, D.; McGehee, M. D.; Karunadasa, H. I. A Layered Hybrid Perovskite Solar-Cell Absorber with Enhanced Moisture Stability. *Angew. Chem., Int. Ed.* **2014**, *53*, 11232−11235.
(89) Milot, R. L.; Sutton, R. J.; Eperon, G. E.; Haghighirad, A. A.; Martinez Hardigree, J. M.; Miranda, L.; Snaith, H. J.; Johnston, M. B.; Herz, L. M. Charge-Carrier Dynamics in 2D Hybrid Metal−Halide Perovskites. *Nano Lett.* **2016**, *16*, 7001−7007.
(90) Sichert, J. A.; Tong, Y.; Mutz, N.; Vollmer, M.; Fischer, S.; Milowska, K. Z.; García Cortadella, R. G.; Nickel, B.; Cardenas-Daw, C.; Stolarczyk, J. K.; Urban, A. S.; Feldmann, J. Quantum Size Effect in Organometal Halide Perovskite Nanoplatelets. *Nano Lett.* **2015**, *15*, 6521−6527.
(91) Kumar, S.; Jagielski, J.; Yakunin, S.; Rice, P.; Chiu, Y.-C.; Wang, M.; Nedelcu, G.; Kim, Y.; Lin, S.; Santos, E. J. G.; Kovalenko, M. V.; Shih, C.-J. Efficient Blue Electroluminescence Using Quantum-Confined Two-Dimensional Perovskites. *ACS Nano* **2016**, *10*, 9720−9729.
(92) Weidman, M. C.; Seitz, M.; Stranks, S. D.; Tisdale, W. A. Highly Tunable Colloidal Perovskite Nanoplatelets through Variable Cation, Metal, and Halide Composition. *ACS Nano* **2016**, *10*, 7830−7839.
(93) Katan, C.; Mercier, N.; Even, J. Quantum and Dielectric Confinement Effects in Lower-Dimensional Hybrid Perovskite Semiconductors. *Chem. Rev.* **2019**, *119*, 3140−3192.
(94) Cho, K. T.; Grancini, G.; Lee, Y.; Oveisi, E.; Ryu, J.; Almora, O.; Tschumi, M.; Schouwink, P. A.; Seo, G.; Heo, S.; Park, J.; Jang, J.; Paek, S.; Garcia-Belmonte, S.; Nazeeruddin, M. K. Selective growth of layered perovskites for stable and efficient photovoltaics. *Energy Environ. Sci.* **2018**, *11*, 952−959.
(95) Wang, N.; Cheng, L.; Ge, R.; Zhang, S.; Miao, Y.; Zou, W.; Yi, C.; Sun, Y.; Cao, R.; Yang, R.; Wei, Y.; Guo, Q.; Ke, Y.; Yu, M.; Jin, Y.; Liu, Y.; Ding, Q.; Di, D.; Yang, L.; Xing, G.; Tian, H.; Jin, C.; Gao, F.; Friend, R. H.; Wang, J.; Huang, W. Perovskite light-emitting diodes based on solution-processed self-organized multiple quantum wells. *Nat. Photonics* **2016**, *10*, 699−704.
(96) Seo, J.-Y.; Choi, J.; Kim, H.-S.; Kim, J.; Yang, J.-M.; Cuhadar, C.; Han, J. S.; Kim, S.-J.; Lee, D.; Jang, H. W.; Park, N.-G. Wafer-scale reliable switching memory based on 2-dimensional layered organic−inorganic halide perovskite. *Nanoscale* **2017**, *9*, 17144−17144.
(97) Feng, J.; Gong, C.; Gao, H.; Wen, W.; Gong, Y.; Jiang, X.; Zhang, B.; Wu, Y.; Wu, Y.; Fu, H.; Jiang, L.; Zhang, X. Single-crystalline layered metal-halide perovskite nanowires for ultrasensitive photodetectors. *Nat. Electron.* **2018**, *1*, 404−410.
(98) Dou, L.; Wong, A. B.; Yu, Y.; Lai, M.; Kornienko, N.; Eaton, S. W.; Fu, A.; Bischak, C. G.; Ma, J.; Ding, T.; Ginsberg, N. S.; Wang, L.-W.; Alivisatos, A. P.; Yang, P. Atomically thin two-dimensional organic-inorganic hybrid perovskites. *Science* **2015**, *349*, 1518−1521.
(99) Yuan, M.; Quan, L. N.; Comin, R.; Walters, G.; Sabatini, R.; Voznyy, O.; Hoogland, S.; Zhao, Y.; Beauregard, E. M.; Kanjanaboos, P.; Lu, Z.; Kim, D. H.; Sargent, E. H. Perovskite energy funnels for efficient light-emitting diodes. *Nat. Nanotechnol.* **2016**, *11*, 872−877.
(100) Ling, Y.; Yuan, Z.; Tian, Y.; Wang, X.; Wang, J. C.; Xin, Y.; Hanson, K.; Ma, B.; Gao, H. Bright Light-Emitting Diodes Based on Organometal Halide Perovskite Nanoplatelets. *Adv. Mater.* **2016**, *28*, 305−311.
(101) Zhao, B.; Bai, S.; Kim, V.; Lamboll, R.; Shivanna, R.; Auras, F.; Richter, J. M.; Yang, L.; Dai, L.; Alsari, M.; She, X.-J.; Liang, L.; Zhang, J.; Lilliu, S.; Gao, P.; Snaith, H. J.; Wang, J.; Greenham, N. C.; Friend, R. H.; Di, D. High-efficiency perovskite−polymer bulk heterostructure light-emitting diodes. *Nat. Photonics* **2018**, *12*, 783−789.
(102) Yang, X.; Zhang, X.; Deng, J.; Chu, Z.; Jiang, Q.; Meng, J.; Wang, P.; Zhang, L.; Yin, Z.; You, J. Efficient green light-emitting diodes based on quasi-two-dimensional composition and phase engineered perovskite with surface passivation. *Nat. Commun.* **2018**, *9*, 570.
(103) Titkov, I. E.; Karpov, S. Y.; Yadav, A.; Mamedov, D.; Zerova, V. L.; Rafailov, E. Efficiency of True-Green Light Emitting Diodes: Non-Uniformity and Temperature Effects. *Materials* **2017**, *10*, 1323.
(104) Nie, W.; Tsai, H.; Asadpour, R.; Blancon, J.-C.; Neukirch, A. J.; Gupta, G.; Crochet, J. J.; Chhowalla, M.; Tretiak, S.; Alam, M. A.; Wang, H.-L.; Mohite, A. D. High-efficiency solution-processed perovskite solar cells with millimeter-scale grains. *Science* **2015**, *347*, 522−525.
(105) Wang, Z.; Lin, Q.; Chmiel, F. P.; Sakai, N.; Herz, L. M.; Snaith, H. J. Efficient ambient-air-stable solar cells with 2D−3D heterostructured butylammonium-caesium-formamidinium lead halide perovskites. *Nat. Energy* **2017**, *2*, 17135.
(106) Liu, Y.; Akin, S.; Pan, L.; Uchida, R.; Arora, N.; Milić, J. V.; Hinderhofer, A.; Schreiber, F.; Uhl, A. R.; Zakeeruddin, S. M.; Hagfeldt, A.; Dar, M. I.; Grätzel, M. Ultrahydrophobic 3D/2D fluoroarene bilayer-based water-resistant perovskite solar cells with efficiencies exceeding 22%. *Sci. Adv.* **2019**, *5*, eaaw2543.
(107) Kwon, K. C.; Hong, K.; Van Le, Q.; Lee, S. Y.; Choi, J.; Kim, K.-B.; Kim, S. Y.; Jang, H. W. Inhibition of Ion Migration for Reliable Operation of Organolead Halide Perovskite-Based Metal/Semiconductor/Metal Broadband Photodetectors. *Adv. Funct. Mater.* **2016**, *26*, 4213−4222.
(108) Tyagi, P.; Arveson, S. M.; Tisdale, W. A. Colloidal Organohalide Perovskite Nanoplatelets Exhibiting Quantum Confinement. *J. Phys. Chem. Lett.* **2015**, *6*, 1911−1916.
(109) Saparov, B.; Mitzi, D. B. Organic−Inorganic Perovskites: Structural Versatility for Functional Materials Design. *Chem. Rev.* **2016**, *116*, 4558−4596.
(110) Zhang, Q.; Su, R.; Liu, X.; Xing, J.; Sum, T. C.; Xiong, Q. High-Quality Whispering-Gallery-Mode Lasing from Cesium Lead Halide Perovskite Nanoplatelets. *Adv. Funct. Mater.* **2016**, *26*, 6238−6245.
(111) Niu, W.; Eiden, A.; Vijaya Prakash, G.; Baumberg, J. J. Exfoliation of self-assembled 2D organic-inorganic perovskite semiconductors. *Appl. Phys. Lett.* **2014**, *104*, 171111.
(112) Wang, G.; Li, D.; Cheng, H.-C.; Li, Y.; Chen, C.-Y.; Yin, A.; Zhao, Z.; Lin, Z.; Wu, H.; He, Q.; Ding, M.; Liu, Y.; Huang, Y.; Duan, X. Wafer-scale growth of large arrays of perovskite microplate crystals for functional electronics and optoelectronics. *Sci. Adv.* **2015**, *1*, e1500613.

https://dx.doi.org/10.1021/acs.jpcc.0c06868
J. Phys. Chem. C 2020, 124, 21895−21908

(113) Shi, E.; Gao, Y.; Finkenauer, B. P.; Akriti; Coffey, A. H.; Dou, L. Two-dimensional halide perovskite nanomaterials and heterostructures. *Chem. Soc. Rev.* **2018**, *47*, 6046−6072.
(114) Lan, C.; Zhou, Z.; Wei, R.; Ho, J. C. Two-dimensional perovskite materials: From synthesis to energy-related applications. *Mater. Today Energy* **2019**, *11*, 61−82.
(115) Hintermayr, V. A.; Richter, A. F.; Ehrat, F.; Döblinger, M.; Vanderlinden, W.; Sichert, J. A.; Tong, Y.; Polavarapu, L.; Feldmann, J.; Urban, A. S. Tuning the Optical Properties of Perovskite Nanoplatelets through Composition and Thickness by Ligand-Assisted Exfoliation. *Adv. Mater.* **2016**, *28*, 9478−9485.
(116) Protesescu, L.; Yakunin, S.; Bodnarchuk, M. I.; Krieg, F.; Caputo, R.; Hendon, C. H.; Yang, R. X.; Walsh, A.; Kovalenko, M. V. Nanocrystals of Cesium Lead Halide Perovskites ($CsPbX_3$, X = Cl, Br, and I): Novel Optoelectronic Materials Showing Bright Emission with Wide Color Gamut. *Nano Lett.* **2015**, *15*, 3692−3696.
(117) Swarnkar, A.; Marshall, A. R.; Sanehira, E. M.; Chernomordik, B. D.; Moore, D. T.; Christians, J. A.; Chakrabarti, T.; Luther, J. M. Quantum dot−induced phase stabilization of α-$CsPbI_3$ perovskite for high-efficiency photovoltaics. *Science* **2016**, *354*, 92−95.
(118) Wu, C.; Wu, T.; Yang, Y.; McLeod, J. A.; Wang, Y.; Zou, Y.; Zhai, T.; Li, J.; Ban, M.; Song, T.; Gao, X.; Duhm, S.; Sirringhaus, H.; Sun, B. Alternative Type Two-Dimensional−Three-Dimensional Lead Halide Perovskite with Inorganic Sodium Ions as a Spacer for High-Performance Light-Emitting Diodes. *ACS Nano* **2019**, *13*, 1645−1654.
(119) Yakunin, S.; Protesescu, L.; Krieg, F.; Bodnarchuk, M. I.; Nedelcu, G.; Humer, M.; De Luca, G.; Fiebig, M.; Heiss, W.; Kovalenko, M. V. Low-threshold amplified spontaneous emission and lasing from colloidal nanocrystals of caesium lead halide perovskites. *Nat. Commun.* **2015**, *6*, 8056.
(120) Wang, Y.; Li, X.; Song, J.; Xiao, L.; Zeng, H.; Sun, H. All-Inorganic Colloidal Perovskite Quantum Dots: A New Class of Lasing Materials with Favorable Characteristics. *Adv. Mater.* **2015**, *27*, 7101−7108.
(121) Chiba, T.; Hayashi, Y.; Ebe, H.; Hoshi, K.; Sato, J.; Sato, S.; Pu, Y.-J.; Ohisa, S.; Kido, J. Anion-exchange red perovskite quantum dots with ammonium iodine salts for highly efficient light-emitting devices. *Nat. Photonics* **2018**, *12*, 681−687.
(122) Bekenstein, Y.; Koscher, B. A.; Eaton, S. W.; Yang, P.; Alivisatos, A. P. Highly Luminescent Colloidal Nanoplates of Perovskite Cesium Lead Halide and Their Oriented Assemblies. *J. Am. Chem. Soc.* **2015**, *137*, 16008−16011.
(123) Akkerman, Q. A.; Motti, S. G.; Srimath Kandada, A. R.; Mosconi, E.; D'Innocenzo, V.; Bertoni, G.; Marras, S.; Kamino, B. A.; Miranda, L.; De Angelis, F.; Petrozza, A.; Prato, M.; Manna, L. Solution Synthesis Approach to Colloidal Cesium Lead Halide Perovskite Nanoplatelets with Monolayer-Level Thickness Control. *J. Am. Chem. Soc.* **2016**, *138*, 1010−1016.
(124) Shamsi, J.; Dang, Z.; Bianchini, P.; Canale, C.; Di Stasio, F.; Brescia, R.; Prato, M.; Manna, L. Colloidal Synthesis of Quantum Confined Single Crystal $CsPbBr_3$ Nanosheets with Lateral Size Control up to the Micrometer Range. *J. Am. Chem. Soc.* **2016**, *138*, 7240−7243.
(125) Pan, A.; He, B.; Fan, X.; Liu, Z.; Urban, J. J.; Alivisatos, A. P.; He, L.; Liu, Y. Insight into the Ligand-Mediated Synthesis of Colloidal $CsPbBr_3$ Perovskite Nanocrystals: The Role of Organic Acid, Base, and Cesium Precursors. *ACS Nano* **2016**, *10*, 7943−7954.
(126) Tong, Y.; Ehrat, F.; Vanderlinden, W.; Cardenas-Daw, C.; Stolarczyk, J. K.; Polavarapu, L.; Urban, A. S. Dilution-Induced Formation of Hybrid Perovskite Nanoplatelets. *ACS Nano* **2016**, *10*, 10936−10944.
(127) Weidman, M. C.; Goodman, A. J.; Tisdale, W. A. Colloidal Halide Perovskite Nanoplatelets: An Exciting New Class of Semiconductor Nanomaterials. *Chem. Mater.* **2017**, *29*, 5019−5030.
(128) Ha, S. K.; Mauck, C. M.; Tisdale, W. A. Toward Stable Deep-Blue Luminescent Colloidal Lead Halide Perovskite Nanoplatelets: Systematic Photostability Investigation. *Chem. Mater.* **2019**, *31*, 2486−2496.
(129) Li, J.; Luo, L.; Huang, H.; Ma, C.; Ye, Z.; Zeng, J.; He, H. 2D Behaviors of Excitons in Cesium Lead Halide Perovskite Nanoplatelets. *J. Phys. Chem. Lett.* **2017**, *8*, 1161−1168.
(130) Bohn, B. J.; Tong, Y.; Gramlich, M.; Lai, M. L.; Döblinger, M.; Wang, K.; Hoye, R. L. Z.; Müller-Buschbaum, P.; Stranks, S. D.; Urban, A. S.; Polavarapu, L.; Feldmann, J. Boosting Tunable Blue Luminescence of Halide Perovskite Nanoplatelets through Post-synthetic Surface Trap Repair. *Nano Lett.* **2018**, *18*, 5231−5238.
(131) Shamsi, J.; Kubicki, D.; Anaya, M.; Liu, Y.; Ji, K.; Frohna, K.; Grey, C. P.; Friend, R. H.; Stranks, S. D. Stable Hexylphosphonate-Capped Blue-Emitting Quantum-Confined $CsPbBr_3$ Nanoplatelets. *ACS Energy Lett.* **2020**, *5*, 1900−1907.
(132) Tong, Y.; Bladt, E.; Aygüler, M. F.; Manzi, A.; Milowska, K. Z.; Hintermayr, V. A.; Docampo, P.; Bals, S.; Urban, A. S.; Polavarapu, L.; Feldmann, J. *Angew. Chem., Int. Ed.* **2016**, *55*, 13887−13892.
(133) Mir, W. J.; Jagadeeswararao, M.; Das, S.; Nag, A. Colloidal Mn-Doped Cesium Lead Halide Perovskite Nanoplatelets. *ACS Energy Lett.* **2017**, *2*, 537−543.
(134) Bertolotti, F.; Nedelcu, G.; Vivani, A.; Cervellino, A.; Masciocchi, N.; Guagliardi, A.; Kovalenko, M. V. Crystal Structure, Morphology, and Surface Termination of Cyan-Emissive, Six-Monolayers-Thick $CsPbBr_3$ Nanoplatelets from X-ray Total Scattering. *ACS Nano* **2019**, *13*, 14294−14307.
(135) Yang, D.; Zou, Y.; Li, P.; Liu, Q.; Wu, L.; Hu, H.; Xu, Y.; Sun, B.; Zhang, Q.; Lee, S.-T. Large-scale synthesis of ultrathin cesium lead bromide perovskite nanoplates with precisely tunable dimensions and their application in blue light-emitting diodes. *Nano Energy* **2018**, *47*, 235−242.
(136) Shynkarenko, Y.; Bodnarchuk, M. I.; Bernasconi, C.; Berezovska, Y.; Verteletskyi, V.; Ochsenbein, S. T.; Kovalenko, M. V. Direct Synthesis of Quaternary Alkylammonium-Capped Perovskite Nanocrystals for Efficient Blue and Green Light-Emitting Diodes. *ACS Energy Lett.* **2019**, *4*, 2703−2711.
(137) Liu, X.; Yu, D.; Cao, F.; Li, X.; Ji, J.; Chen, J.; Song, X.; Zeng, H. Low-Voltage Photodetectors with High Responsivity Based on Solution-Processed Micrometer-Scale All-Inorganic Perovskite Nanoplatelets. *Small* **2017**, *13*, 1700364.
(138) Lee, C.; Wei, X.; Kysar, J. W.; Hone, J. Measurement of the Elastic Properties and Intrinsic Strength of Monolayer Graphene. *Science* **2008**, *321*, 385−388.
(139) Wang, L.; Meric, I.; Huang, P. Y.; Gao, Q.; Gao, Y.; Tran, H.; Taniguchi, T.; Watanabe, K.; Campos, L. M.; Muller, D. A.; Guo, J.; Kim, P.; Hone, J.; Shepard, K. L.; Dean, C. R. One-Dimensional Electrical Contact to a Two-Dimensional Material. *Science* **2013**, *342*, 614−617.
(140) Yang, F.; Song, P.; Ruan, M.; Xu, W. Recent progress in two-dimensional nanomaterials: Synthesis, engineering, and applications. *Flatchem* **2019**, *18*, 100133.
(141) Wang, Q. H.; Kalantar-Zadeh, K.; Kis, A.; Coleman, J. N.; Strano, M. S. Electronics and optoelectronics of two-dimensional transition metal dichalcogenides. *Nat. Nanotechnol.* **2012**, *7*, 699−712.
(142) Choi, W.; Choudhary, N.; Han, G. H.; Park, J.; Akinwande, D.; Lee, Y. H. Recent development of two-dimensional transition metal dichalcogenides and their applications. *Mater. Today* **2017**, *20*, 116−130.
(143) Hinnemann, B.; Moses, P. G.; Bonde, J.; Jørgensen, K. P.; Nielsen, J. H.; Horch, S.; Chorkendorff, I.; Nørskov, J. K. Biomimetic Hydrogen Evolution: MoS_2 Nanoparticles as Catalyst for Hydrogen Evolution. *J. Am. Chem. Soc.* **2005**, *127*, 5308−5309.
(144) Das, P.; Fu, Q.; Bao, X.; Wu, Z.-S. Recent advances in the preparation, characterization, and applications of two-dimensional heterostructures for energy storage and conversion. *J. Mater. Chem. A* **2018**, *6*, 21747−21784.
(145) Cao, X.; Tan, C.; Zhang, X.; Zhao, W.; Zhang, H. Solution-Processed Two-Dimensional Metal Dichalcogenide-Based Nanomaterials for Energy Storage and Conversion. *Adv. Mater.* **2016**, *28*, 6167−6196.

https://dx.doi.org/10.1021/acs.jpcc.0c06868
J. Phys. Chem. C 2020, 124, 21895−21908

(146) Chang, K.; Chen, W. L-Cysteine-Assisted Synthesis of Layered MoS_2/Graphene Composites with Excellent Electrochemical Performances for Lithium Ion Batteries. *ACS Nano* **2011**, *5*, 4720−4728.
(147) Xu, X.; Rout, C. S.; Yang, J.; Cao, R.; Oh, P.; Shin, H. S.; Cho, J. Freeze-dried WS_2 composites with low content of graphene as high-rate lithium storage materials. *J. Mater. Chem. A* **2013**, *1*, 14548−14554.
(148) Su, D.; Dou, S.; Wang, G. WS_2@graphene nanocomposites as anode materials for Na-ion batteries with enhanced electrochemical performances. *Chem. Commun.* **2014**, *50*, 4192−4195.
(149) Ma, L.; Zhou, X.; Xu, L.; Xu, X.; Zhang, L.; Chen, W. Ultrathin few-layered molybdenum selenide/graphene hybrid with superior electrochemical Li-storage performance. *J. Power Sources* **2015**, *285*, 274−280.
(150) Radisavljevic, B.; Radenovic, A.; Brivio, J.; Giacometti, V.; Kis, A. Single-layer MoS_2 transistors. *Nat. Nanotechnol.* **2011**, *6*, 147−150.
(151) Huang, L.; Wei, Q.; Xu, X.; Shi, C.; Liu, X.; Zhou, L.; Mai, L. Methyl-functionalized MoS_2 nanosheets with reduced lattice breathing for enhanced pseudocapacitive sodium storage. *Phys. Chem. Chem. Phys.* **2017**, *19*, 13696−13702.
(152) Xu, Y.; Yan, L.; Li, X.; Xu, X. Fabrication of transition metal dichalcogenides quantum dots based on femtosecond laser ablation. *Sci. Rep.* **2019**, *9*, 2931.
(153) Liu, K.-K.; Zhang, W.; Lee, Y.-H.; Lin, Y.-C.; Chang, M.-T.; Su, C.-Y.; Chang, C.-S.; Li, H.; Shi, Y.; Zhang, H.; Lai, C.-S.; Li, L.-J. Growth of Large-Area and Highly Crystalline MoS2 Thin Layers on Insulating Substrates. *Nano Lett.* **2012**, *12*, 1538−1544.
(154) Nicolosi, V.; Chhowalla, M.; Kanatzidis, M. G.; Strano, M. S.; Coleman, J. N. Liquid Exfoliation of Layered Materials. *Science* **2013**, *340*, 1226419.
(155) Coleman, J. N.; Lotya, M.; O'Neill, A.; Bergin, S. D.; King, P. J.; Khan, U.; Young, K.; Gaucher, A.; De, S.; Smith, R. J.; Shvets, I. V.; Arora, S. K.; Stanton, G.; Kim, H.-Y.; Lee, K.; Kim, G. T.; Duesberg, G. S.; Hallam, T.; Boland, J. J.; Wang, J. J.; Donegan, J. F.; Grunlan, J. C.; Moriarty, G.; Shmeliov, A.; Nicholls, R. J.; Perkins, J. M.; Grieveson, E. M.; Theuwissen, K.; McComb, D. W.; Nellist, P. D.; Nicolosi, V. Two-Dimensional Nanosheets Produced by Liquid Exfoliation of Layered Materials. *Science* **2011**, *331*, 568−571.
(156) Zeng, Z.; Yin, Z.; Huang, X.; Li, H.; He, Q.; Lu, G.; Boey, F.; Zhang, H. Single-Layer Semiconducting Nanosheets: High-Yield Preparation and Device Fabrication. *Angew. Chem., Int. Ed.* **2011**, *50*, 11093−11097.
(157) Yoo, D.; Kim, M.; Jeong, S.; Han, J.; Cheon, J. Chemical Synthetic Strategy for Single-Layer Transition-Metal Chalcogenides. *J. Am. Chem. Soc.* **2014**, *136*, 14670−14673.
(158) Mahler, B.; Hoepfner, V.; Liao, K.; Ozin, G. A. Colloidal Synthesis of 1T-WS_2 and 2H-WS_2 Nanosheets: Applications for Photocatalytic Hydrogen Evolution. *J. Am. Chem. Soc.* **2014**, *136*, 14121−14127.
(159) Ramakrishna Matte, H. S. S.; Gomathi, A.; Manna, A. K.; Late, D. J.; Datta, R.; Pati, S. K.; Rao, C. N. R. MoS_2 and WS_2 Analogues of Graphene. *Angew. Chem., Int. Ed.* **2010**, *49*, 4059−4062.
(160) Altavilla, C.; Sarno, M.; Ciambelli, P. A Novel Wet Chemistry Approach for the Synthesis of Hybrid 2D Free-Floating Single or Multilayer Nanosheets of MS_2@oleylamine (M═Mo, W). *Chem. Mater.* **2011**, *23*, 3879−3885.
(161) Zhang, X.; Lai, Z.; Tan, C.; Zhang, H. Solution-Processed Two-Dimensional MoS_2 Nanosheets: Preparation, Hybridization, and Applications. *Angew. Chem., Int. Ed.* **2016**, *55*, 8816−8838.
(162) Han, J. H.; Kwak, M.; Kim, Y.; Cheon, J. Recent Advances in the Solution-Based Preparation of Two-Dimensional Layered Transition Metal Chalcogenide Nanostructures. *Chem. Rev.* **2018**, *118*, 6151−6188.
(163) Xiao, J.; Wang, X.; Yang, X.-Q.; Xun, S.; Liu, G.; Koech, P. K.; Liu, J.; Lemmon, J. P. Electrochemically Induced High Capacity Displacement Reaction of PEO/MoS_2/Graphene Nanocomposites with Lithium. *Adv. Funct. Mater.* **2011**, *21*, 2840−2846.
(164) Jaramillo, T. F.; Jørgensen, K. P.; Bonde, J.; Nielsen, J. H.; Horch, S.; Chorkendorff, I. Identification of Active Edge Sites for Electrochemical H_2 Evolution from MoS_2 Nanocatalysts. *Science* **2007**, *317*, 100−102.
(165) Huang, X.; Zeng, Z.; Bao, S.; Wang, M.; Qi, X.; Fan, Z.; Zhang, H. Solution-phase epitaxial growth of noble metal nanostructures on dispersible single-layer molybdenum disulfide nanosheets. *Nat. Commun.* **2013**, *4*, 1444.
(166) Yuwen, L.; Xu, F.; Xue, B.; Luo, Z.; Zhang, Q.; Bao, B.; Su, S.; Weng, L.; Huang, W.; Wang, L. General synthesis of noble metal (Au, Ag, Pd, Pt) nanocrystal modified MoS_2 nanosheets and the enhanced catalytic activity of Pd−MoS_2 for methanol oxidation. *Nanoscale* **2014**, *6*, 5762−5769.
(167) Xu, X.; Fan, Z.; Ding, S.; Yu, D.; Du, Y. Fabrication of MoS_2 nanosheet@TiO_2 nanotube hybrid nanostructures for lithium storage. *Nanoscale* **2014**, *6*, 5245−5250.
(168) Chen, Y.; Song, B.; Tang, X.; Lu, L.; Xue, J. Ultrasmall Fe_3O_4 Nanoparticle/MoS_2 Nanosheet Composites with Superior Performances for Lithium Ion Batteries. *Small* **2014**, *10*, 1536−1543.
(169) Chen, J.; Wu, X.-J.; Yin, L.; Li, B.; Hong, X.; Fan, Z.; Chen, B.; Xue, C.; Zhang, H. One-pot Synthesis of CdS Nanocrystals Hybridized with Single-Layer Transition-Metal Dichalcogenide Nanosheets for Efficient Photocatalytic Hydrogen Evolution. *Angew. Chem., Int. Ed.* **2015**, *54*, 1210−1214.
(170) Chou, S. S.; Kaehr, B.; Kim, J.; Foley, B. M.; De, M.; Hopkins, P. E.; Huang, J.; Brinker, C. J.; Dravid, V. P. Chemically Exfoliated MoS_2 as Near-Infrared Photothermal Agents. *Angew. Chem., Int. Ed.* **2013**, *52*, 4160−4164.
(171) Perkins, F. K.; Friedman, A. L.; Cobas, E.; Campbell, P. M.; Jernigan, G. G.; Jonker, B. T. Chemical Vapor Sensing with Monolayer MoS_2. *Nano Lett.* **2013**, *13*, 668−673.
(172) Lee, K.; Kim, H.-Y.; Lotya, M.; Coleman, J. N.; Kim, G.-T.; Duesberg, G. S. Electrical Characteristics of Molybdenum Disulfide Flakes Produced by Liquid Exfoliation. *Adv. Mater.* **2011**, *23*, 4178−4182.
(173) Connor, B. A.; Leppert, L.; Smith, M. D.; Neaton, J. B.; Karunadasa, H. I. Layered Halide Double Perovskites: Dimensional Reduction of $Cs_2AgBiBr_6$. *J. Am. Chem. Soc.* **2018**, *140*, 5235−5240.
(174) Zhang, X.-Q.; Lin, C.-H.; Tseng, Y.-W.; Huang, K.-H.; Lee, Y.-H. Synthesis of Lateral Heterostructures of Semiconducting Atomic Layers. *Nano Lett.* **2015**, *15*, 410−415.
(175) Tang, G.; You, P.; Tai, Q.; Yang, A.; Cao, J.; Zheng, F.; Zhou, Z.; Zhao, J.; Chan, P. K. L.; Yan, F. Solution-Phase Epitaxial Growth of Perovskite Films on 2D Material Flakes for High-Performance Solar Cells. *Adv. Mater.* **2019**, *31*, 1807689.
(176) Klimov, V. I.; Mikhailovsky, A. A.; Xu, S.; Malko, A.; Hollingsworth, J. A.; Leatherdale, A. C.; Eisler, H.-J.; Bawendi, M. G. Optical Gain and Stimulated Emission in Nanocrystal Quantum Dots. *Science* **2000**, *290*, 314−317.
(177) Li, Q.; Lian, T. Area- and Thickness-Dependent Biexciton Auger Recombination in Colloidal CdSe Nanoplatelets: Breaking the "Universal Volume Scaling Law. *Nano Lett.* **2017**, *17*, 3152−3158.
(178) Guzelturk, B.; Pelton, M.; Olutas, M.; Demir, H. V. Giant Modal Gain Coefficients in Colloidal II−VI Nanoplatelets. *Nano Lett.* **2019**, *19*, 277−282.
(179) Moreels, I. Let There Be Order, in Films of Colloidal CdSe 2D Nanocrystals. *Nano Lett.* **2020**, *20*, 2941−2942.
(180) Cunningham, P. D.; Coropceanu, I.; Mulloy, K.; Cho, W.; Talapin, D. V. Quantized Reaction Pathways for Solution Synthesis of Colloidal ZnSe Nanostructures: A Connection between Clusters, Nanowires, and Two-Dimensional Nanoplatelets. *ACS Nano* **2020**, *14*, 3847−3857.
(181) Blankenship, R. E.; Tiede, D. M.; Barber, J.; Brudvig, G. W.; Fleming, G.; Ghirardi, M.; Gunner, M. R.; Junge, W.; Kramer, D. M.; Melis, A.; Moore, T. A.; Moser, C. C.; Nocera, D. G.; Nozik, A. J.; Ort, D. R.; Parson, W. W.; Prince, R. C.; Sayre, R. T. Comparing Photosynthetic and Photovoltaic Efficiencies and Recognizing the Potential for Improvement. *Science* **2011**, *332*, 805−809.
(182) Lewis, N. S.; Nocera, D. G. Powering the planet: Chemical challenges in solar energy utilization. *Proc. Natl. Acad. Sci. U. S. A.* **2006**, *103*, 15729−15735.

https://dx.doi.org/10.1021/acs.jpcc.0c06868
J. Phys. Chem. C 2020, 124, 21895−21908

(183) Philbin, J. P.; Rabani, E. Electron−Hole Correlations Govern Auger Recombination in Nanostructures. *Nano Lett.* **2018**, *18*, 7889−7895.
(184) Li, Q.; Zhou, B.; McBride, J. R.; Lian, T. Efficient Diffusive Transport of Hot and Cold Excitons in Colloidal Type II CdSe/CdTe Core/Crown Nanoplatelet Heterostructures. *ACS Energy Lett.* **2017**, *2*, 174−181.
(185) Li, Q.; Lian, T. Exciton dissociation dynamics and light-driven H_2 generation in colloidal 2D cadmium chalcogenide nanoplatelet heterostructures. *Nano Res.* **2018**, *11*, 3031−3049.
(186) Sigle, D. O.; Zhang, L.; Ithurria, S.; Dubertret, B.; Baumberg, J. J. Ultrathin CdSe in Plasmonic Nanogaps for Enhanced Photocatalytic Water Splitting. *J. Phys. Chem. Lett.* **2015**, *6*, 1099−1103.
(187) Stolarczyk, J. K.; Bhattacharyya, S.; Polavarapu, L.; Feldmann, J. Challenges and Prospects in Solar Water Splitting and CO_2 Reduction with Inorganic and Hybrid Nanostructures. *ACS Catal.* **2018**, *8*, 3602−3635.
(188) Zhukovskyi, M.; Tongying, P.; Yashan, H.; Wang, Y.; Kuno, M. Efficient Photocatalytic Hydrogen Generation from Ni Nanoparticle Decorated CdS Nanosheets. *ACS Catal.* **2015**, *5*, 6615−6623.
(189) Mongin, C.; Garakyaraghi, S.; Razgoniaeva, N.; Zamkov, M.; Castellano, F. N. Direct observation of triplet energy transfer from semiconductor nanocrystals. *Science* **2016**, *351*, 369−372.
(190) Wu, M.; Congreve, D. N.; Wilson, M. W. B.; Jean, J.; Geva, N.; Welborn, M.; Van Voorhis, T.; Bulovic, V.; Bawendi, M. G.; Baldo, M. A. Solid-state infrared-to-visible upconversion sensitized by colloidal nanocrystals. *Nat. Photonics* **2016**, *10*, 31−34.
(191) Kholmicheva, N.; Budkina, D. S.; Cassidy, J.; Porotnikov, D.; Harankahage, D.; Boddy, A.; Galindo, M.; Khon, D.; Tarnovsky, A. N.; Zamkov, M. Sustained Biexciton Populations in Nanoshell Quantum Dots. *ACS Photonics* **2019**, *6*, 1041−1050.
(192) Razgoniaeva, N.; Moroz, P.; Yang, M.; Budkina, D. S.; Eckard, H.; Augspurger, M.; Khon, D.; Tarnovsky, A. N.; Zamkov, M. One-Dimensional Carrier Confinement in "Giant" CdS/CdSe Excitonic Nanoshells. *J. Am. Chem. Soc.* **2017**, *139*, 7815−7822.
(193) Razgoniaeva, N.; Yang, M.; Colegrove, C.; Kholmicheva, N.; Moroz, P.; Eckard, H.; Vore, A.; Zamkov, M. Double-Well Colloidal Nanocrystals Featuring Two-Color Photoluminescence. *Chem. Mater.* **2017**, *29*, 7852−7858.
(194) Pokatilov, E. P.; Fonoberov, V. A.; Fomin, V. M.; Devreese, J. T. Electron and hole states in quantum dot quantum wells within a spherical eight-band model. *Phys. Rev. B: Condens. Matter Mater. Phys.* **2001**, *64*, 245329.
(195) Braun, M.; Link, S.; Burda, C.; El-Sayed, M. Transfer times of electrons and holes across the interface in CdS/HgS/CdS quantum dot quantum well nanoparticles. *Chem. Phys. Lett.* **2002**, *361*, 446−452.
(196) Battaglia, D.; Li, J. J.; Wang, Y.; Peng, X. Colloidal Two-Dimensional Systems: CdSe Quantum Shells and Wells. *Angew. Chem., Int. Ed.* **2003**, *42*, 5035−5039.
(197) Singldinger, A.; Gramlich, M.; Gruber, C.; Lampe, C.; Urban, A. S. Nonradiative Energy Transfer between Thickness-Controlled Halide Perovskite Nanoplatelets. *ACS Energy Lett.* **2020**, *5*, 1380−1385.
(198) Li, C.; Zang, Z.; Han, C.; Hu, Z.; Tang, X.; Du, J.; Leng, Y.; Sun, K. Highly compact $CsPbBr_3$ perovskite thin films decorated by ZnO nanoparticles for enhanced random lasing. *Nano Energy* **2017**, *40*, 195−202.
(199) Ma, C.; Clark, S.; Liu, Z.; Liang, L.; Firdaus, Y.; Tao, R.; Han, A.; Liu, X.; Li, L.-J.; Anthopoulos, T. D.; Hersam, M. C.; Wu, T. Solution-Processed Mixed-Dimensional Hybrid Perovskite/Carbon Nanotube Electronics. *ACS Nano* **2020**, *14*, 3969−3979.
(200) Ma, C.; Shi, Y.; Hu, W.; Chiu, M.-H.; Liu, Z.; Bera, A.; Li, F.; Wang, H.; Li, L.-J.; Wu, T. Heterostructured $WS_2/CH_3NH_3PbI_3$ Photoconductors with Suppressed Dark Current and Enhanced Photodetectivity. *Adv. Mater.* **2016**, *28*, 3683−3689.
(201) Pan, A.; Jurow, M.; Zhao, Y.; Qiu, F.; Liu, Y.; Yang, J.; Urban, J. J.; He, L.; Liu, Y. Templated self-assembly of one-dimensional $CsPbX_3$ perovskite nanocrystal superlattices. *Nanoscale* **2017**, *9*, 17688−17693.
(202) Giustino, F.; Snaith, H. J. Toward Lead-Free Perovskite Solar Cells. *ACS Energy Lett.* **2016**, *1*, 1233−1240.
(203) Slavney, A. H.; Hu, T.; Lindenberg, A. M.; Karunadasa, H. I. A Bismuth-Halide Double Perovskite with Long Carrier Recombination Lifetime for Photovoltaic Applications. *J. Am. Chem. Soc.* **2016**, *138*, 2138−2141.
(204) Yu, J. H.; Lee, H. R.; Hong, S. S.; Kong, D.; Lee, H.-W.; Wang, H.; Xiong, F.; Wang, S.; Cui, Y. Vertical Heterostructure of Two-Dimensional MoS_2 and WSe_2 with Vertically Aligned Layers. *Nano Lett.* **2015**, *15*, 1031−1035.
(205) Wang, P.-P.; Sun, H.; Ji, Y.; Li, W.; Wang, X. Three-Dimensional Assembly of Single-Layered MoS_2. *Adv. Mater.* **2014**, *26*, 964−969.

https://dx.doi.org/10.1021/acs.jpcc.0c06868
J. Phys. Chem. C 2020, 124, 21895−21908